This is the accepted manuscript (postprint) of the following article:
Nazari, A., & Eslami-Farsani, R. (2025). A review of photothermal and superhydrophobic polymer nanocomposites as anti-icing nanocoatings. *Polymer Composites*, *46*(6), 5018-5040.
https://doi.org/10.1002/pc.29305

A review of photothermal and superhydrophobic polymer nanocomposites as anti-icing nanocoatings

Ali Nazari[1], Reza Eslami-Farsani[1*]

[1]Faculty of Materials Science and Engineering, K. N. Toosi University of Technology, Tehran, Iran.

[*] Corresponding author: eslami@kntu.ac.ir

Abstract

Freezing and ice formation at low temperatures have always caused numerous challenges in variant crafts such as aeronautical, transportation, power lines, oil platforms, etc. Anti-icing and de-icing approaches have been employed to reduce the contrary results of icing on surfaces. Due to the disadvantages of de-icing methods, anti-icing techniques are noteworthy, and extensive research has been done in this field. Anti-icing techniques have been used to prevent ice accumulation or simplify separating once the ice has formed. Superhydrophobicity has the property that can neglect to ice or delay icing on the surface. Nowadays, nanocomposites, one of the most extremely used advanced substances, are used in various industries and usages. In the meantime, polymer nanocomposites as a nanocoating offer innovative solutions for the icing phenomenon by bridging the areas of polymer composite technology, nanoscience, and superhydrophobicity. Additionally, photothermal polymer nanocomposites are based on conventional superhydrophobic materials with high solar absorption rates and have unique anti-icing properties. In this review, the types of ice were examined in terms of their appearance, formation order, and crystal structure. Also, various theories of wettability and freezing mechanisms were studied. Moreover, various methods of making surface superhydrophobic such as top-down, and bottom-top procedures were mentioned. Finally, superhydrophobic and photothermal polymer nanocomposite coatings were explained in-depth.

Highlights

- Types of ice and its structure were investigated.
- kinds of wettability theories and freezing mechanisms were studied.
- Methods of ice formation prevention were summarized.
- Superhydrophobic and photothermal polymer nanocomposites were explained.

This is the accepted manuscript (postprint) of the following article:
Nazari, A., & Eslami-Farsani, R. (2025). A review of photothermal and superhydrophobic polymer nanocomposites as anti-icing nanocoatings. *Polymer Composites*, *46*(6), 5018-5040.
https://doi.org/10.1002/pc.29305

Keywords: Advanced materials, Polymer nanocomposite, Nanocoating, Icing mechanism, Wettability theory, Superhydrophobicity, Photothermal.

1. Introduction

Icing is a widespread natural occurrence. Ice accretion poses a safety risk for various modes of transportation, including aircraft, wind turbines, very fast-movement rail, power lines, offshore oil platforms, and other infrastructure and systems. This icing phenomenon can create significant hazards that must be addressed.[1-6] Anti-icing and de-icing approaches have been employed to reduce the contrary effects of freezing on surfaces which can be active or passive.

The active de-icing strategy involves using chemical, heating, thermoelectric, electromagnetic, or mechanical methods to wipe ice stacked on surfaces.[7-11] For example, the electromagnetic-impulsive de-icing technique acts by inducing powerful and abrupt magnetic forces from a high direct-current pulse through a coil, causing quick acceleration and curvature of the icing surface. This leads to detachment and elimination of the ice. These methods have been found to work victoriously in the aviation industry.[7] Elsewhere, using motorized cutters for scraping ice on a ship is regularly feasible only after an icing storm. It is rarely conceivable to manually scrape ice from the upper parts of the structures that are the most decretive sections for a ship's stability.[9] Active de-icing systems, while actively addressing ice removal, also have inherent drawbacks. These include high power consumption, abstruse and uninterrupted maintenance requirements, an accretion in overall system weight, and the need to reapply chemicals repeatedly. These negative factors associated with active de-icing systems can lead to increased design, fabrication, and operational costs, as well as significant negative environmental consequences. So, while active de-icing methods are helpful, they also come with their own set of challenges and downsides that need to be carefully considered.[12-14]

Active anti-icing methods also have disadvantages such as high energy consumption, system complexity, the need for continuous maintenance, and in some cases, the use of toxic substances. These negative factors associated with active anti-icing systems can lead to an increase in design, construction, and operation costs as well as significant negative environmental consequences.[14]

In the passive anti-icing methods, the formation of ice on the surface is prevented without using external energy. Also, in the passive de-icing methods, the ice is destroyed without using external energy. passive anti-icing techniques have been used to prevent ice accumulation or simplify segregation once the ice has been formed Considering the disadvantages mentioned in the active de-icing and active anti-icing methods, nowadays the use of passive anti-icing and passive de-icing methods is very meaningful, and extensive research has been done in this field.[15-26]

Zhu et al,[16] produced a multipurpose cement concrete blend by blending "cool cold" black tints with cement, sand, TiO_2 nanobits, and water. After the blending had been mortared on a cement

This is the accepted manuscript (postprint) of the following article:
Nazari, A., & Eslami-Farsani, R. (2025). A review of photothermal and superhydrophobic polymer nanocomposites as anti-icing nanocoatings. *Polymer Composites*, *46*(6), 5018-5040.
https://doi.org/10.1002/pc.29305

concrete sheet, evaporated at room temperature, and treated with fluorine silicon sol, a gray cement concrete leaf was attained. Simultaneously, the "cool cold" cement concrete superhydrophobe surface depicted imperial anti-ice efficiency. Also, Wang et al,[23] to meliorate the anti-freezing efficiency of asphalt pedestrians and deduce the impression of pedestrian icing, adopted the technique of anti-clotting ice coating on the surface of asphalt pavement. In this study, usage investigation relied on an anti-clotting ice-veneer substance on asphalt pedestrians using standard test techniques. With various amounts of anti-clotting ice agent, the primary efficiency indexes, containing the icing temperature and ice adherence on the veneer surface, of anti-clotting ice veneer material were contrasted. In another research, Dong et al,[24] explored a hot-air scruff-heating technique for the anti-freezing mechanism of a little aero-engine cone, as well as experimental research on its efficiency. Tests were directed under various icing circumstances and hot air parameters in a freezing wind tunnel, using a full-scale empirical cone pattern of a little aero-engine. The temperature dispensations on the cone surface were meted by thermocouples. Test outcomes represented that the hot-air blanket anti-freezing technique is impressive for the cone leading edge. Likewise exhibited was a scalar simulation of the temperature dispensations of the aero-engine cone under freezing circumstances. The flow area near the cone was attained by calculative fluid dynamics code. The pathways of supercooled water globs and the gathering performance were computed using the Lagrangian approximate. The mate outcomes of heat and mass conveyance were observed in the temperature calculation of the cone. The heat analysis model noted the mass equilibrium of water and energy equilibrium on the face of the cone. The simulation outcomes were contrasted with the experimental considerations. The specifications of the hot-air blanket heating anti-freezing technique were likewise studied.

Nowadays, polymer nanocomposites, as a group of advanced materials have received much attention in different crafts and sciences because of their unparalleled characteristics.[27-32] Moreover, polymer nanocomposites are a new generation of anti-freezing veneers that provide an innovative solution to deal with the challenges of icing.[33] This group of nanocoatings has many advantages such as enhanced thermal insulation, improved mechanical properties, increased surface hydrophobicity, self-healing capability, and environmental stability.[34-38] This importance has caused many empirical and numerical articles and research to be done in this field.[39]

First, this review explains the taxonomies of ice based on formation mechanisms and the taxonomies of ice based on appearance. Then, surface wettability theories and icing mechanisms are explored. In the following, making superhydrophobic surfaces (top-down, bottom-up, and concoction of bottom-up and top-down techniques) as anti-icing methods are discussed. Finally, types of polymer nanocomposites, such as superhydrophobic and photothermal nanocomposites, are discussed and investigated as a pioneering anti-icing method to prevent ice accumulation on surfaces.

This is the accepted manuscript (postprint) of the following article:
Nazari, A., & Eslami-Farsani, R. (2025). A review of photothermal and superhydrophobic polymer nanocomposites as anti-icing nanocoatings. *Polymer Composites*, *46*(6), 5018-5040.
https://doi.org/10.1002/pc.29305

2. Types of ice and its formation mechanisms

2.1. Types of ice

2.1.1. Classifications of ice based on formation mechanism

Ice is a general term used for freezing water substances. There are three types of icing based on the freezing mechanism as follows[40-42]:

- Sedimentation icing: This type of icing is developed by freezing rain or falling snow grains on the surface at a temperature of 0 ºC or less. In this condition, the super-cold temperature for ice formation has an inverse relationship with the size of the water droplets. For example, larger drops have a lower super-cold temperature. The super-cold temperature in fog drops can be more than 10 ºC. One of the types of ice formed in this group is glaze ice, which is very dangerous due to its robustness and high density.

- Cloud icing (in-cloud icing): In this instance, freezing occurs because of the contact of the super-cold nebula with the surface. In these conditions, there is no snow or rain, and the degree of freezing depends on factors such as humidity and airflow speed. The small size of the fog droplets causes the latent heat in them to be released quickly and ice to form. The type of ice is rime in this case.

- Deposition icing: It is a type of frost that creates as an outcome of direct freezing of water vapor on the surface. It does not have a large volume, and because it has weak adhesion, it is easily separated from the surface.

2.1.2. Classifications of ice based on the appearance

Based on the density, and physical appearance, icing can be categorized as glazed ice, granular rime, crystalline rime, wet snow, and mixed rime.

- Glazed ice: it has a glassy and transparent appearance, a hard and unbreakable texture, and a density between 0.6 g/cm^3 and 0.9 g/cm^3. It also has very high adhesion and is considered the most dangerous type of frostbite.

- Granular rime: It has a dull ivory color, and its density is between 0.1 g/cm^3 and 0.3 g/cm^3. It has a loose and layered texture that includes air bubbles, which makes it have a wavy and irregular surface.

- Crystalline rime: They have a crystalline appearance and many bubbles inside. They have a soft texture and density between 0.01 g/cm^3 and 0.08 g/cm^3 and are easily separated from the surface.

- Wet snow: its color is dull ivory white and has a soft texture with a density between 0.1 g/cm^3 and 0.7 g/cm^3. This type is created when the snow on the surface turns into ice due to the continuous decrease in temperature.

This is the accepted manuscript (postprint) of the following article:
Nazari, A., & Eslami-Farsani, R. (2025). A review of photothermal and superhydrophobic polymer nanocomposites as anti-icing nanocoatings. *Polymer Composites*, *46*(6), 5018-5040.
https://doi.org/10.1002/pc.29305

- Mixed rime: It has an ivory white color, large size with many bubbles, which is created by alternating glaze and rime freezing on the surface, and its density is between 0.2 g/cm^3 and 0.6 g/cm^3.

In general, the temperature of ice formation on the surface is relatively higher (-10 ºC), which also has high adhesion. On the other hand, rime is created at lower temperatures (less than -20 ºC), which does not get a chance to escape due to the super-fast freezing of air bubbles, which causes its adhesion to the surface to weaken.[43-45] Figure 1(a) shows the probability of glaze and rime formation at different altitudes according to humidity, temperature, and pressure quantities.[46] Also, Figures 1(b) and 1(c) show the appearance of glaze and rime respectively.[40]

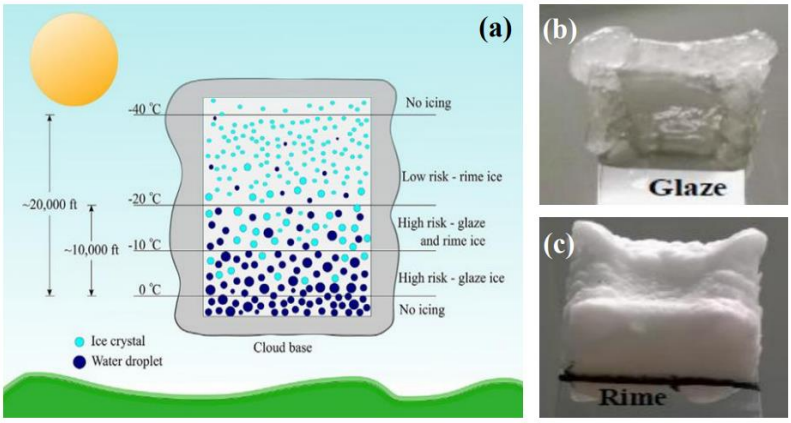

Figure 1. Schematics of, a) Glaze and rime formation conditions,[46] b) Glaze, c) Rime.[40]

2.1.3. Classifications of ice based on the crystal structures

Icing or freezing of water is a phase transformation from a liquid state (water) to a solid state (ice) under a super cold temperature of ΔT (difference between melting temperature and actual freezing temperature). Figure 2 is related to the phase diagram of water. As can be seen, the physical properties of water, such as melting point and boiling point, change significantly with the change of pressure. Also, the crystal form of ice is different in various parts of the diagram. There are more than 10 different crystal structures of ice at different temperatures and pressures. All ice crystal structures include one water molecule that has hydrogen bonds with four other water molecules. Among the various forms of ice, hexagonal ice, and cubic ice are the most common. Hexagonal ice is the most common natural state for ice and snow on Earth. Cubic ice is generally formed in the Earth's atmosphere and extraterrestrial environments. Also, it can be the preferred phase for ice formation, resulting from tiny water droplets at a very low temperature. In addition, cubic ice can be an intermediate phase in the path of ice nucleation in heterogeneous conditions.[47]

This is the accepted manuscript (postprint) of the following article:
Nazari, A., & Eslami-Farsani, R. (2025). A review of photothermal and superhydrophobic polymer nanocomposites as anti-icing nanocoatings. *Polymer Composites*, *46*(6), 5018-5040.
https://doi.org/10.1002/pc.29305

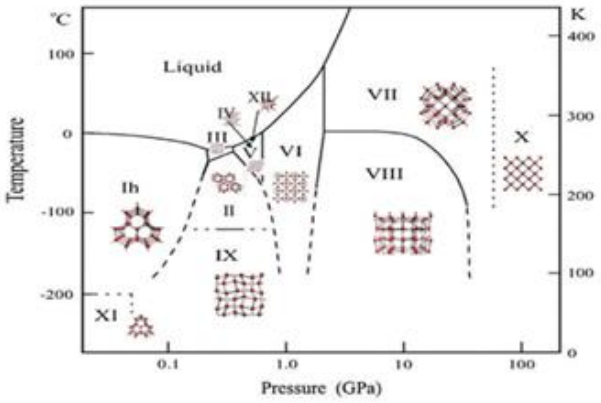

Figure 2. Water phase diagram.[47]

2.2. Surface wettability theories

The wetting phenomenon arises from the interactions amongst gas, liquid, and solid phases at the molecular level. The relationship between adhesive and cohesive forces influences the amount of wetting. One key parameter in assessing the wettability of solid surfaces is the contact angle. A larger contact angle indicates a more hydrophobic surface, which reduces the likelihood of ice formation. The wettability behavior of a solid surface is related to surface tension and surface topography parameters.[48]

According to the surface topography in static conditions, the connection between the contact angle and interfacial energies is defined by three equations, which vary based on surface characteristics and the type of interfacial boundary.[49-54] The first equation is Young's equation, which is reliable for plain, chemically neutral, and equivalent surfaces (Figure 3-a) and is calculated from equation (1).[55,56]

$$cos\theta_Y = (\gamma_{SA} - \gamma_{SL})/\gamma_{LA} \quad (1)$$

In which θ_Y is the contact angle of the liquid glob in equilibrium with the surface. γ_{SA}, γ_{SL}, and γ_{LA} are the surface tension of the solid-gas, solid-liquid, and liquid-gas boundaries, correspondingly.

The second equation is called Wenzel, which is related to surfaces with roughness and equivalent conditions where water globs penetrate between the surface roughness. Equation (2) represents this relation (Figure 3-b).[57]

$$cos\theta_W = r(\gamma_{SA} - \gamma_{SL})/\gamma_{LA} = rcos\theta_Y \quad (2)$$

Here θ_W is Wenzel angle, and r is the harshness factor of the surface.

The third correlation is Cassie-Baxter (Figure 3-c), which is related to surfaces with roughness and heterogeneous conditions. In the Cassie-Baxter model, the water glob remains on top of

This is the accepted manuscript (postprint) of the following article:
Nazari, A., & Eslami-Farsani, R. (2025). A review of photothermal and superhydrophobic polymer nanocomposites as anti-icing nanocoatings. *Polymer Composites*, *46*(6), 5018-5040.
https://doi.org/10.1002/pc.29305

the surface asperities with none entering the spaces within the micro-nano array. Additionally, air cavities are captured in the gaps of this harsh structure, which decreases the touch domain between the water and the solid surface. The Cassie-Baxter angle can be computed using equation (3).[58]

$$cos\theta_{CB} = f_1 cos\theta_1 + f_2 cos\theta_2 \quad (3)$$

Here θ_{CB} is the Cassie-Baxter apparent contact angle. f_1 and f_2 are fractions of the contact surface in phases 1 and 2, and θ_1 and θ_2 are the contact angles with phases 1 and 2, respectively.

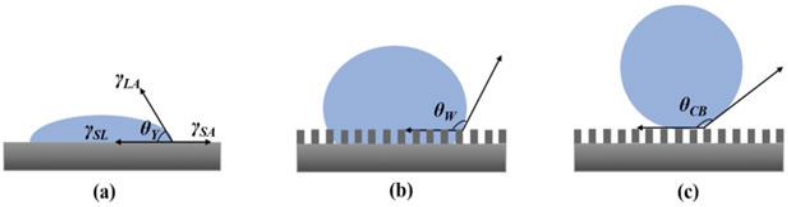

Figure 3. Illustration of methodical wetting formats, a) Young state, b) Wenzel state, c) Cassie-Baxter state.[51]

So far, the mentioned laws have been related to static conditions, for dynamic conditions (Figure 4), the Furmidge equation (4) is used.[59]

$$mgsin\alpha = \omega\gamma^{la}(cos\theta_r - cos\theta_a) \quad (4)$$

In which mg is the weight of the drop, ω is the diameter of the wetted surface. γ^{la} is the liquid-air interfacial free energy, and α is the rolling angle (at least the angle at which the drop starts to roll on the slope surface). θ_a is the advancing contact angle, θ_r is the receding contact angle, and the disagreement between θ_a and θ_r angles are defined as the contact angle hysteresis (CAH).

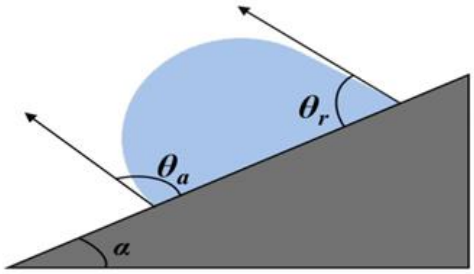

Figure 4. Illustration of rolling angle and contact angle in dynamic state.[56]

This is the accepted manuscript (postprint) of the following article:
Nazari, A., & Eslami-Farsani, R. (2025). A review of photothermal and superhydrophobic polymer nanocomposites as anti-icing nanocoatings. *Polymer Composites*, *46*(6), 5018-5040.
https://doi.org/10.1002/pc.29305

According to equation (4), low CAH is an indication of the simple movement of the water glob over the surface and increasing the superhydrophobicity.[59]

Yang, Wenzel, and Cassie-Baxter investigated the wettability based on surface topography conditions. But in fact, the most efficient method to predict and determine the amount of wettability is to check the amount of Gibbs free energy (GFE), so that by reducing it, wettability decreases. Two interfaces are important in wettability and contact angle. The first is the solid-liquid interface and the second is the liquid-vapor interface. In many articles, the liquid-vapor interface is assumed to be a smooth surface without curvature to simplify calculations. To more accurately calculate the amount of wettability, the value of the curvature of the liquid-vapor interface should be taken into account.[60] Marmur,[61] provided a more accurate formula for the wettability of the solid surface by considering the curvature of the liquid-vapor interface. To check the value of the water contact angle (WCA), Marmur assumed that water droplets have a constant volume and also that the size of the water droplet is much bigger than the size of the surface roughness (Figure 3). The equilibrium shape of the drop is a spherical cap, so to derive the relationships, the equations of the sphere have been used. GFE can be calculated from equation (5).

$$G = \gamma_{LA}A_{LA} + \gamma_{SL}A_{SL} + \gamma_{SA}A_{SA} \quad (5)$$

Here A is the interfacial area and G is Gibbs free energy.

According to the spherical cap shape of the drop, the solid-liquid area can be calculated from equation (6).

$$A_{SL} = r_f f \pi R^2 . sin^2\theta \quad (6)$$

Here R is the radius of the spherical cap of a droplet, θ is the apparent contact angle, r_f is the roughness ratio of the wetted area, and f is the fraction of the projected area of the solid-liquid interface.

The liquid-gas interface consists of two parts. The first part is outside the spherical cap interface (between gas and liquid) and the second part is the liquid-gas interface inside the surface roughness, which can be calculated through equation (7) (Figure 5).

$$A_{LA} = 2\pi R^2(1 - \cos\theta) + r'_{f'}\pi R^2 . sin^2\theta \quad (7)$$

where $r'_{f'}$ is the roughness ratio of the interface between the liquid and gas phases, and f' is the liquid-gas interface projected area fraction.

This is the accepted manuscript (postprint) of the following article:
Nazari, A., & Eslami-Farsani, R. (2025). A review of photothermal and superhydrophobic polymer nanocomposites as anti-icing nanocoatings. *Polymer Composites*, *46*(6), 5018-5040.
https://doi.org/10.1002/pc.29305

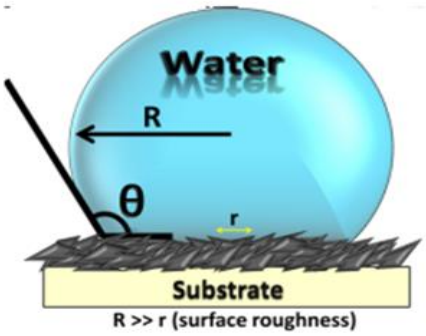

Figure 5. Illustration of a water droplet on a rough solid film.[60]

The solid-gas interface also includes two parts, the solid-gas interface inside the surface roughness and the interface outside the drop, which is obtained from equation (8).

$$A_{SA} = A_{total} - A_{SL} \quad (8)$$

Here A_{total} is the total area of the solid surface.

By inserting equations 6, 7, and 8 in equation 5, the relationship for determining the amount of G is obtained (equation 9).

$$G = \gamma_{LA}\,[2\pi R^2\,(1 - \cos\theta)] + [\gamma_{LA} r'_{f'} f' + (\gamma_{SL} - \gamma_{SA}) r_f f]\pi R^2 \quad (9)$$

Here A_{total} is constant and does not affect the GFE reduction. Equation (9) can be used for all types of solid surfaces with any material or surface topography.

2.3. Icing mechanism

Ice is a crystalline solid, and is created by converting the phases of liquid water or water vapor into a solid phase. Freezing begins with the germination of ice nuclei and continues with the development of resistant nuclei until the freezing process is complete. During this process, as outlined by the second law of thermodynamics, disordered water vapor or liquid water molecules, which possess high entropy, are converted into more ordered molecules that exhibit lower entropy (crystalline solid ice). In this scenario, an energy barrier needs to be surpassed, which can be achieved through supersaturation or by lowering the temperature significantly. This free energy barrier (ΔG) for ice nucleation is calculated by equation (10).[62-64]

$$\Delta G = \pi\sigma_{lv} {r_0}^2 (2 - 3cos\theta + cos\theta^3)/3 \quad (10)$$

Here σ_{lv} refers to the liquid-vapor surface energy, while r_0 represents the critical radius, as defined by Kelvin's classical equation (11).[65]

$$\ln\left(\frac{p}{p_\infty}\right) = 2\sigma_{lv}/n_l kTr_0 \quad (11)$$

This is the accepted manuscript (postprint) of the following article:
Nazari, A., & Eslami-Farsani, R. (2025). A review of photothermal and superhydrophobic polymer nanocomposites as anti-icing nanocoatings. *Polymer Composites*, *46*(6), 5018-5040.
https://doi.org/10.1002/pc.29305

In equation (11), p is the gas pressure, and p_∞ is the equilibrium gas pressure of the condensed phase at temperature T. k is the Boltzmann constant, and n_l is the number of molecules per unit volume of the liquid phase.

If the radius of the initial ice seed surpasses the critical radius, a stable ice core is created, and its sudden growth happens.[66] Ice grows by water molecules on the ice crystal surface and is controlled by heat conveyance from the water-ice boundary.[67] In actual conditions, because of the presence of pollutants in the air and their deposition on the solid surface, heterogeneous germination is generally created. In this condition, ice core germination is easier.[68,69] Schematics of the ice formation mechanism and ice crystal growth process are illustrated in Figure 6.[70]

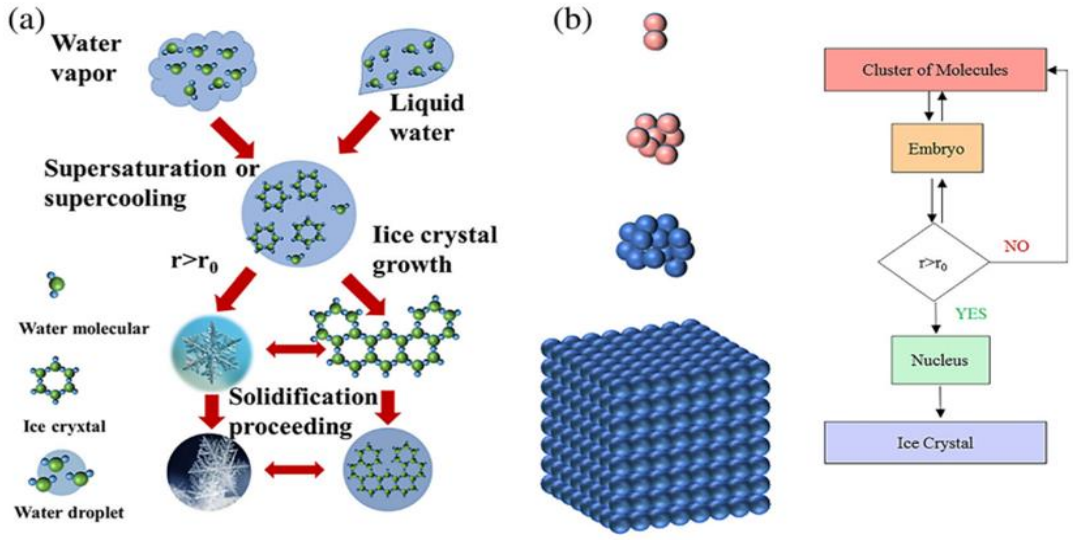

Figure 6. Schematic illustrations of, a) mechanism of ice formation, b) the process of ice crystal growth.[70]

Ice nucleation inside a water glob is called homogeneous ice nucleation, whereas heterogeneous ice nucleation happens at the solid-liquid interface. Heterogeneous nucleation is more beneficial on hydrophilic surfaces than on superhydrophobic surfaces because of the greater contact area between the water glob and the hydrophilic solid surface.[71] Homogeneous nucleation can be improved by introducing surface harshness with nanoparticle radii less than ten times the size of the critical ice nuclei.[72,73] As a result, icephobic surfaces can be engineered by facilitating homogeneous nucleation, which accounts for the -25 °C ice nucleation temperature of water on a surface, while utilizing high nucleation energy.[74-76]

In particular, the icing phenomenon on a solid surface is a complex physical process involving simultaneous phase transition and heat transfer. When using a superhydrophobic anti-icing material, the unique surface structure causes droplets to maintain a spherical shape upon contact. This allows the droplets to easily roll off the material's surface. As a result, the water droplets rapidly escape before they can freeze, effectively preventing ice formation and

This is the accepted manuscript (postprint) of the following article:
Nazari, A., & Eslami-Farsani, R. (2025). A review of photothermal and superhydrophobic polymer nanocomposites as anti-icing nanocoatings. *Polymer Composites*, *46*(6), 5018-5040.
https://doi.org/10.1002/pc.29305

achieving anti-icing before it occurs. During the icing process, the low wettability of water droplets combined with the superhydrophobic surface results in a minimal contact area between the droplets and the interface. This prevents the droplets from penetrating the micro-nano structure, allowing some air with low thermal conductivity to remain trapped between them. This gas layer reduces heat transfer, raises the energy barrier for ice nucleation, and slows down the rate at which ice crystals form, effectively controlling the icing speed. Furthermore, as previously mentioned, ice formation can occur through homogeneous or heterogeneous nucleation. When supercooled water droplets land on regular surfaces like glass, they tend to spread out, leading to homogeneous nucleation and the formation of a solid ice layer that adheres strongly. In contrast, ice nucleation on superhydrophobic surfaces is heterogeneous, starting from the bottom of the spherical droplets and progressing upward to create a spherical ice mass. Although superhydrophobic surfaces significantly delay the freezing time of static droplets, fast-moving droplets can still lead to noticeable ice formation. When water droplets freeze on these surfaces, the limited contact area between the ice and the superhydrophobic material results in weak adhesion. Consequently, the ice layer can easily detach due to its weight, wind, mechanical forces, or external airflow, facilitating de-icing and effectively minimizing large areas of ice accumulation.[48,70]

3. Methods of ice formation prevention

3.1. Make superhydrophobic surface

The first approach to create anti-icing conditions is to create superhydrophobic surfaces to postpone ice creation and decrease the amount of ice adherence to the surface. Both Wenzel's and Cassie–Baxter's laws emphasize that a coarse surface is crucial for increasing hydrophobicity.[77] In actuality, methods for providing superhydrophobic surfaces can primarily be divided into top-down and bottom-up techniques. Top-down methods comprise lithographic and template-based processes,[78] and plasma action as a surface modification technique.[79-89] From the other point of view Bottom-up techniques include self-assembly and self-formation, which are techniques for surface modification.[78,90-98] Instances of bottom-up methods embrace chemical vapor deposition (CVD),[98-104] layer-by-layer (LBL) deposition technique,[90,91,95,98,100] hydrogen grafting,[105] and colloidal aggregations.[78,97,106,107-109] There are likewise techniques based on combining both bottom-up and top-down attitudes, for instance, the foundry of polymer dilution and phase segregation,[110] and electrospinning.[101,111-113]

3.1.1. Top-down procedures

The top-down system is a familiar epithet in microelectronics that describes the process of creating substances and apparatuses by shaping, molding, or machining larger substances using implements and lasers. To create superhydrophobic surfaces, a variety of techniques are utilized, including templating,[114,115] lithographic methods,[116,117,118-121] micromachining,[122] and plasma treatments. Templating, for instance, generally involves a series of steps that include

This is the accepted manuscript (postprint) of the following article:
Nazari, A., & Eslami-Farsani, R. (2025). A review of photothermal and superhydrophobic polymer nanocomposites as anti-icing nanocoatings. *Polymer Composites*, *46*(6), 5018-5040.
https://doi.org/10.1002/pc.29305

molding and replication. After that, the template can be removed by ablation,[106,107] dissolutions,[123] or even sublimation.[124,125] Lithographic methods, on the other hand, involve using light or electron beams to define patterns on a substrate. This technique is highly precise and can produce nanoscale features that contribute to the superhydrophobic virtues of the surface. The desired patterned surfaces are achieved through subsequent etching processes. These surfaces are rendered hydrophobic through a silanization treatment.[116,117,118-121] Micromachining techniques, which include both mechanical and chemical processes, enable the fabrication of complex geometries at a microscale. These methods can be particularly effective in creating surfaces with tailored roughness, which is essential for achieving superhydrophobicity.[122] Lastly, plasma treatments can etch the surface anisotropically and enhance hydrophobic characteristics by rough surface generating. Examples of this include the plasma treatment of polyethylene terephthalate (PET),[87,88] polytetrafluoroethylene (PTFE),[126] and polyethylene (PE).[82] Additionally, pulse-laser behaviors of polydimethylsiloxane (PDMS) have been employed to create superhydrophobic surfaces.[127,128]

3.1.2. Bottom-up procedures

Bottom-up systems focus on creating larger and more intricate objects by combining smaller components or building blocks. In nanofabrication, this approach frequently utilizes self-assembly and self-organization. Self-assembly refers to a process where components naturally come together in a dilution or gas phase, forming a constant structure that minimizes energy. Bottom-up techniques used to make superhydrophobic surfaces encompass variant chemical deposition modes that facilitate the formation of intricate nanostructures. Among these methods, chemical bath deposition (CBD) and CVD stand out for their ability to produce uniform coatings with controlled thickness and composition. CBD involves immersing substrates in a solution containing metal ions, allowing for the gradual deposition of materials through chemical reactions,[89,101,102,104] while CVD utilizes gaseous precursors to deposit thin films on substrates, enabling precise control over the material properties.[101,102] In addition to these methods, electrochemical deposition is another prominent technique that leverages electrochemical reactions to deposit materials onto conductive substrates. This method is particularly advantageous for creating complex geometries and achieving high deposition rates.[98,100,103] Furthermore, LBL deposition techniques, such as electrostatic assembly and colloidal assembly, offer additional avenues for constructing superhydrophobic surfaces. Electrostatic assembly relies on the attraction between oppositely charged materials to build multilayer structures,[90,95] while colloidal assembly utilizes the self-organization of colloidal particles to form ordered arrays.[97,107,109] Sol-gel processes, which involve the transition of a solution into a solid gel phase,[95,106,109,129-140] and hydrogen bonding techniques, which exploit intermolecular forces to assemble materials, also contribute to the versatility of LBL deposition.[105] Chemical synthesis methods further expand the toolkit for creating superhydrophobic surfaces by enabling the design of specific chemical functionalities that enhance water repellency.[141]

This is the accepted manuscript (postprint) of the following article:
Nazari, A., & Eslami-Farsani, R. (2025). A review of photothermal and superhydrophobic polymer nanocomposites as anti-icing nanocoatings. *Polymer Composites*, *46*(6), 5018-5040.
https://doi.org/10.1002/pc.29305

3.1.3. Combination of bottom-up and top-down procedures

Integrating bottom-up and top-down attitudes can leverage the benefits of both orders. This combination is advantageous for developing architectures with dual-scale harshness, similar to that of a lotus leaf. Typically, these combined methods involve two stages: the first stage employs a top-down approach to create a coarse surface, while the second stage utilizes a bottom-up procedure to achieve finer asperity.[142-145] Although, some combination methods may not exhibit a distinct two-stage process.[146,147]

3.2. Polymer nanocomposite coatings

3.2.1. Anti-icing superhydrophobic polymer nanocomposites

Superhydrophobicity has the property that can neglect to ice or delay icing on the surface. Superhydrophobicity can also contain a slipping phenomenon alternative to anti-icing, which reduces ice adherence strength with the surface. The superhydrophobic surface, which has an anti-icing property, is called icephobic. Surfaces, which have high water repellency can prevent ice formation.[148] The water droplet gets dropped off from the surface before freezing on it. This can be said to be the anti-icing property.[149] In a study, it found out that if the roughness is in nano scaling, then there can be a decrease of ice adhesion up to 15 times.[150] Superhydrophobic polymer nanocomposite coatings, created by integrating polymer composite technology, nanoscience, and superhydrophobicity, have proven to be an impressive method for enhancing coating properties.[151] The incorporation of organic and inorganic nanobits, particularly SiO_2,[152,153] carbon nanotubes (CNTs),[154,155] graphene,[156,157] and carbon nanofibers,[158] displays a critical role in the development of these superhydrophobic nanocoatings.

In an investigation done by Sutar et al,[152] a self-cleaning superhydrophobic veneer was created by integrating silica nanoparticles into polymethyl methacrylate (PMMA), achieving a WCA of 165º and a sliding angle of 4º. The researchers noted that the wettability remained stable even after exposure to a vicinal water jet, and the sticking strength was maintained after ten periods of the tape peel experiment. Correspondingly, Ghashghaee et al,[159] developed a stearic acid-modified cupric oxide (CuO)/PMMA nanocomposite veneer that exhibited a WCA of 161º and a sliding angle of 2º. Furthermore, the resulting superhydrophobic coating demonstrated remarkable photocatalytic activity. Photographs of the water droplets on the textile surfaces are illustrated in Figure 7.

This is the accepted manuscript (postprint) of the following article:
Nazari, A., & Eslami-Farsani, R. (2025). A review of photothermal and superhydrophobic polymer nanocomposites as anti-icing nanocoatings. *Polymer Composites*, *46*(6), 5018-5040.
https://doi.org/10.1002/pc.29305

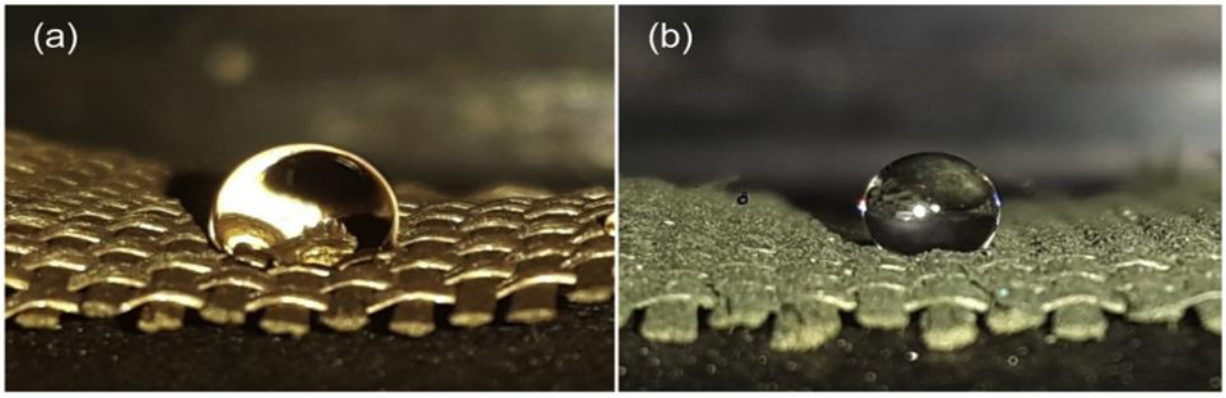

Figure 7. Images of the water glob on, a) the tissue surface coated with the layer of unmodified CuO nanobits and PMMA, b) the tissue surface coated with the layer of modified CuO nanobits and PMMA.[159]

Janowicz et al,[160] developed a superhydrophobic nanocomposite coating that is free from fluorescent materials, utilizing mesoporous silica nanoparticles functionalized with 3-aminopropyl triethoxysilane (APTES) and titanium cross-linked polydimethylsiloxane (Figure 8). This coating achieved a WCA of 168º and a transparency of 90%, leading to excellent adhesion to glass. Researchers utilize a variety of techniques to fabricate superhydrophobic coatings. The main techniques described in this paper are spin coating and aerosol assisted chemical vapor deposition (AACVD), which are illustrated in Figure 9.

This is the accepted manuscript (postprint) of the following article:
Nazari, A., & Eslami-Farsani, R. (2025). A review of photothermal and superhydrophobic polymer nanocomposites as anti-icing nanocoatings. *Polymer Composites*, *46*(6), 5018-5040.
https://doi.org/10.1002/pc.29305

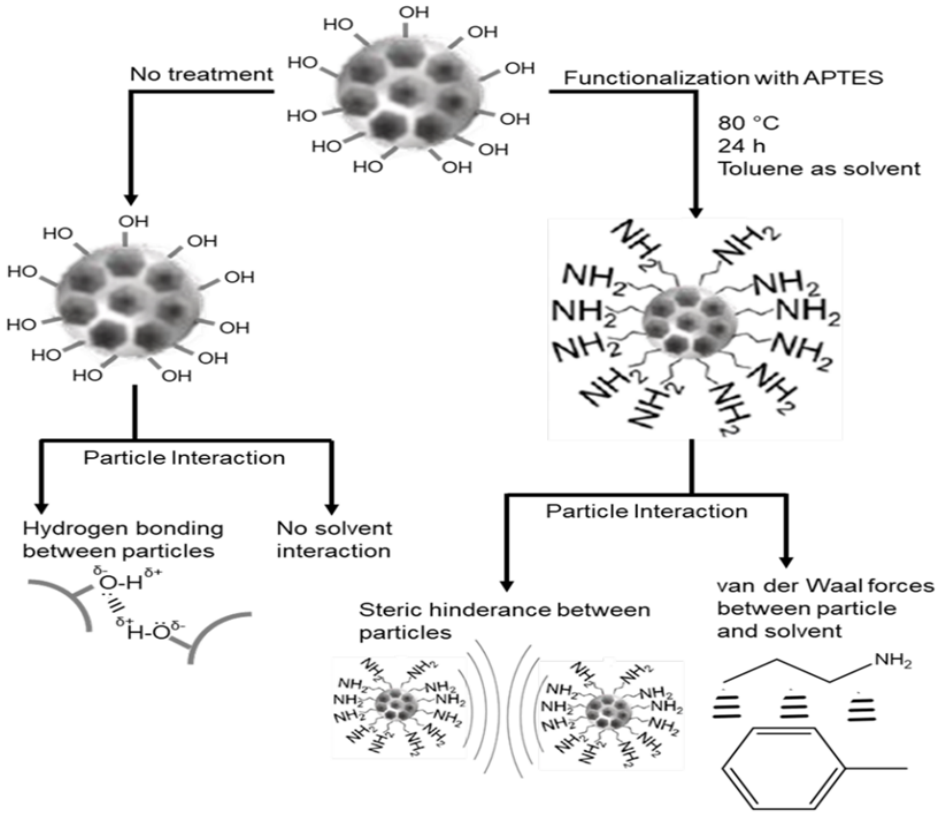

Figure 8. Functionalization of the silica nanoparticles.[160]

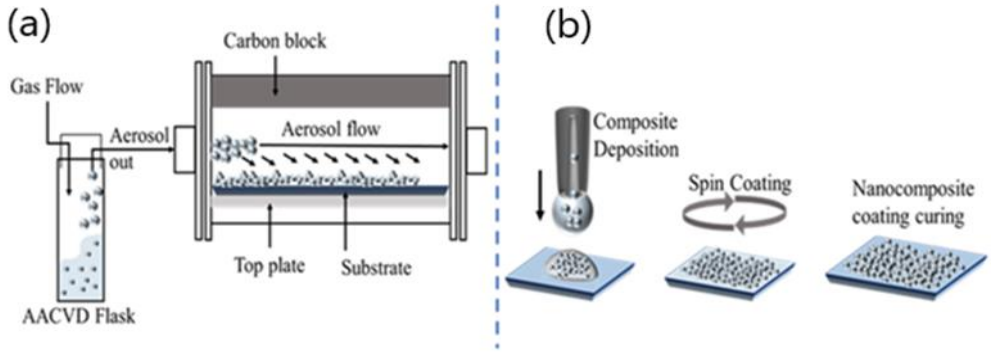

Figure 9. Schematic illustrations of, a) AACVD, b) spin coating procedures.[160]

Wang et al,[161] related to the creation of a graphene composite that exhibits both superhydrophobic and electrothermal properties. This composite effectively prevented ice formation under "glaze ice" conditions by leveraging its superhydrophobic characteristics alongside Joule heating, allowing for surface cleaning and drying without the presence of water droplets. They created a hierarchical arrangement by combining graphene, CNTs, and SiO_2 nanobits, which were combined into the matrix through a process of resolution and

This is the accepted manuscript (postprint) of the following article:
Nazari, A., & Eslami-Farsani, R. (2025). A review of photothermal and superhydrophobic polymer nanocomposites as anti-icing nanocoatings. *Polymer Composites*, *46*(6), 5018-5040.
https://doi.org/10.1002/pc.29305

resolidification. Hydrophobic powders made from graphene, CNT, and SiO_2 were generated by adding additives to an obscure liquid, followed by sonication, magnetic mixture, and applying the last veneer to a glass substrate. After drying, the resulting powder was mixed with ethanol and tetrahydrofuran (THF) and stirred for about two hours. The scanning electron microscopy (SEM) images of composites are shown in Figure 10. Finally, the suspension was used to coat a polycarbonate sheet, which was then dried.

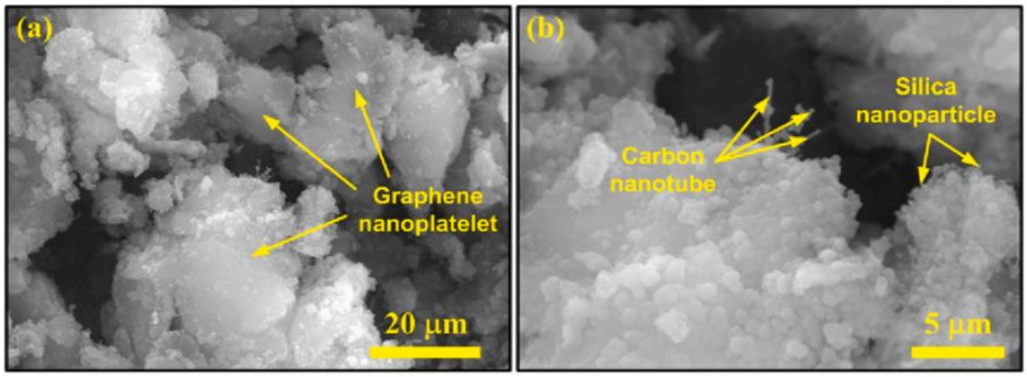

Figure 10. SEM images of the graphene composite at, a) low, b) high magnifications.[161]

In a different study, Wang et al,[162] created a hydrophobic powder and implemented a multi-fluorination approach to develop a superhydrophobic sample. They began by adding PDMS to a dilution of carbon nanofiber in THF. After rousing the mixture, it was combined with a fluorinated curing agent and subjected to ultrasonication, and after that the summation of perfluoropolyether for multi-fluorination. Once the mixture was cast and semi-cured, they evenly spattered the hydrophobic powder onto the face and completed the curing process. Similarly, Peng et al,[163] employed a multi-fluorination strategy to create a veneer using epoxy, perfluoropolyether, polytetrafluoroethylene nanoparticles, and a fluorinated amine curing agent. They applied the suspension onto the substrate using either spraying or roll-coating methods. Furthermore, they chose to conduct the fabrication in aqueous conditions at room temperature, which made the process quick, safe, and straightforward. Zhang et al,[164] reported the creation of a flower-like ZnO/epoxy superhydrophobic coating that exhibits improved durability. They utilized an immersion method for the coating preparation, effectively restoring the superhydrophobic properties compromised by mechanical damage.

3.2.2. Photothermal polymer nanocomposites

Photothermal composite materials build upon traditional superhydrophobic or lubricated surfaces by incorporating photothermal materials with high solar absorption capabilities. The photothermal properties do not alter the original features of the nanocoating. Photothermal substances can be classified by various carbon-based matters that facilitate photothermal conversion, as well as metal nanoparticles like Fe_3O_4 and TiN, along with other semiconductor

This is the accepted manuscript (postprint) of the following article:
Nazari, A., & Eslami-Farsani, R. (2025). A review of photothermal and superhydrophobic polymer nanocomposites as anti-icing nanocoatings. *Polymer Composites*, *46*(6), 5018-5040.
https://doi.org/10.1002/pc.29305

materials.[165] Due to the special properties of photothermal materials and the attractiveness of using them as de-icing and anti-icing coatings, the trend of using them in recent years has been extremely upward (Figure 11).[166]

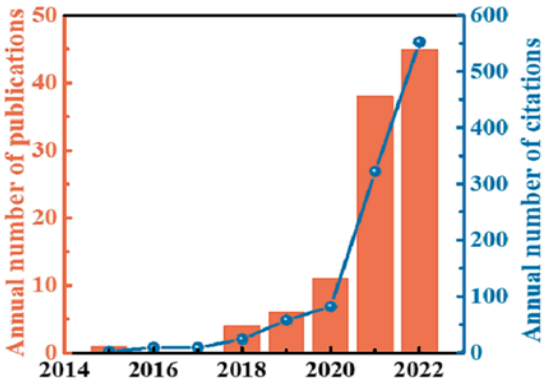

Figure 11. The number of published articles per year indexed in the Web of Science by the title of "photothermal anti-icing/de-icing".[166]

Liu et al,[167] employed silicone oil as a slicking medium, alongside permeable SiO_2 aerogel, CNTs, and a mixture of silicone elastomer and beeswax, to develop a composite self-lubricating coating with a micro-nano conformation that features photo-thermal anti-icing capabilities. Schematic of the fabrication process of the coatings is shown in Figure 12. Their results indicated a WCA of up to 162° and an icing delay of 596 seconds. With just one instance of solar radiance, the skin temperature increased swiftly to 85 °C, allowing ice prisms to melt within 150 seconds. Additionally, the wax as a phase change material, provides the cover with effective self-repairing capabilities. Extreme-black veneers, which are almost fully absorbent, are commonly used in the aerospace, ocular apparatuses, and sun energy sectors. However, the high-temperature circumstances required to prepare extreme-black coatings confine their potential applications.

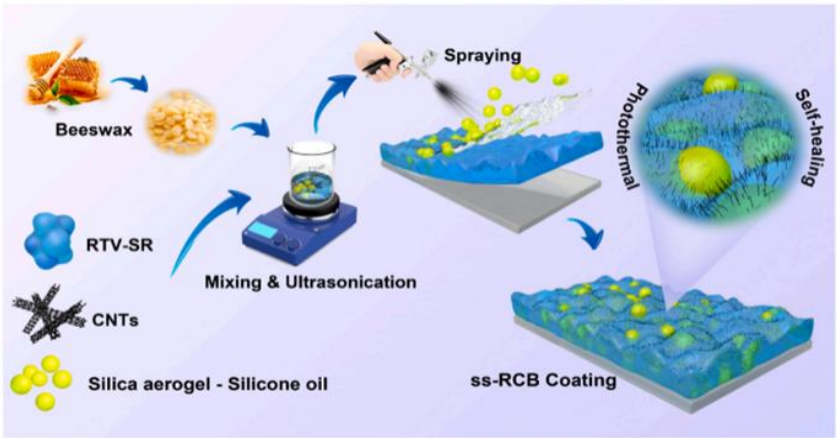

Figure 12. Schematic of the fabrication process of the coatings.[167]

This is the accepted manuscript (postprint) of the following article:
Nazari, A., & Eslami-Farsani, R. (2025). A review of photothermal and superhydrophobic polymer nanocomposites as anti-icing nanocoatings. *Polymer Composites*, *46*(6), 5018-5040.
https://doi.org/10.1002/pc.29305

Additionally, Lin et al,[168] employed laser etching to develop a novel technique for creating CNT/resin composite extreme-black coatings. Using laser etching to omit the absolute resin layer from the veneer's skin, they altered the minimum contact boundary from air/resin to air/CNTs, achieving a maximum mean light absorbance of 99.49%. Concurrently, the planar morphology of the nanocoating transitioned from a plane to a spongy microstructure, resulting in a significant enhancement of photothermal transformation and amended surface harshness and hydrophobicity.

In another study, Yu et al,[169] synthesized a photothermal superhydrophobic polyurethane sponge (PSP-Sponge) consisting of Fe_3O_4 nanoparticles and polydopamine to enable anti-icing and rapid ice removal in low sun irradiation conditions. SEM images of the sponge at different preparation stages are illustrated in Figure 13. Due to the isolation characteristics of the permeable PSP-Sponge, moisture on its surface does not freeze under weak sunlight of 0.3 kW/m² ("0.3 suns") in damp environments at -30 °C. In contrast, subject to "1 sun" disposal, ice can thoroughly fuse within 18 minutes. Furthermore, the sponge exhibits great self-cleaning and self-repairing capabilities, making it resilient in variant and changing natural circumstances, which ensures its durable anti-icing and de-icing effectiveness. In damp outdoor settings at -30 °C, rime on the PSP-Sponge's face can fuse under sunlight equivalent to "0.5 suns." While photothermal materials may experience a reduction in thermal yielding capacity owing to particle waste within use, appropriate substances can be selected to improve or substitute the functionalities of the photothermal bits.

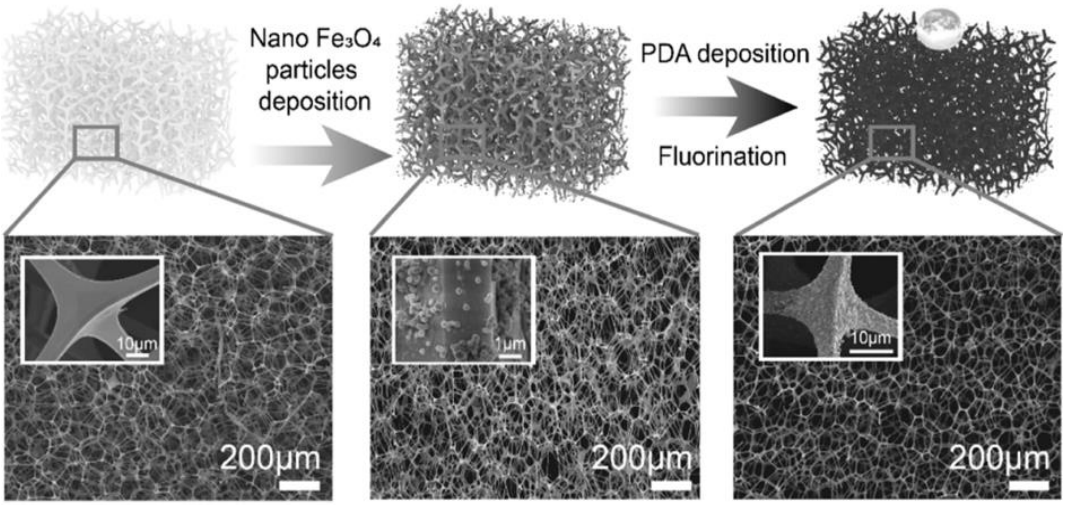

Figure 13. SEM images of PSP-Sponge with high and low-magnification details at different preparation stages.[169]

Likewise, Lee et al,[170] introduced carbonyl iron particles into PDMS to create a magnetically responsive cilia matrix using neodymium magnets. They then applied a top layer of multi-walled carbon nanotubes (MWCNTs) to develop comprehensive anti-freezing coatings

This is the accepted manuscript (postprint) of the following article:
Nazari, A., & Eslami-Farsani, R. (2025). A review of photothermal and superhydrophobic polymer nanocomposites as anti-icing nanocoatings. *Polymer Composites*, *46*(6), 5018-5040.
https://doi.org/10.1002/pc.29305

featuring magnetically responsive photothermal arrays (MRPAs). The MRPA exhibits prompt reversible structural movement when subjected to an exterior magnetic field, allowing it to omit water while maintaining superhydrophobic stability. With over 97.8% absorption, the coating achieves efficient photothermal conversion, resulting in a freezing time of 105 seconds in the lightless condition, with no serious freezing perceived under illuminated circumstances.

In a similar study, Liu et al,[171] synthesized brominated CNTs on the skin of a PDMS layer by grafting 2-perfluoroethyl methacrylate (PFMA). They employed the surface-initiated Cu-controlled radical polymerization (SI-CuCRP) technique to create PFMA/CNTs composite PDMS superhydrophobic coating. After 120 rubs with sandpaper, the PDMS coating maintained a WCA of 170°, demonstrating proper superhydrophobicity and continued dehydration capability. Additionally, it exhibited strong wear stability and self-repairing properties, with freezing time retardation and ice adherence strength measured at 872 seconds and 61.9 kPa, correspondingly, indicating effective anti-freezing capability. Moreover, because of the photothermal transformation capability of CNTs, the PFMA/CNTs composite PDMS superhydrophobic coatings demonstrated superior de-icing effects when subjected to near-infrared irradiation. Deng et al,[172] loaded mesoporous SiO_2 nano pieces ($mSiO_2$) with a vast proportion of PDMS to create hydrophobic PDMS/$mSiO_2$ accumulations (Figure 14). They integrated these aggregates into a silicone matrix along with CNTs to develop an adjacent-infrared reactionary anti-icing/de-icing veneer using a single-stage spraying technique. The PDMS/$mSiO_2$ pieces provided the shield with micro harshness and low surface energy, while the CNTs contributed to making a micro-nano surface, enhancing moisture repellency and adding photothermal properties. As a result, the outcoming veneer exhibited superhydrophobic characteristics with a WCA reaching 154.3°, alongside a freezing delay of 440 seconds at -20 °C, which is almost 73 times longer than that observed on aluminum substrates. Additionally, the finished veneer demonstrated strong adhesion and durable anti-freezing capabilities in severe environmental circumstances, making it a promising solution for enhancing the anti-icing and de-icing performance of rotor wings with durability and resilience.

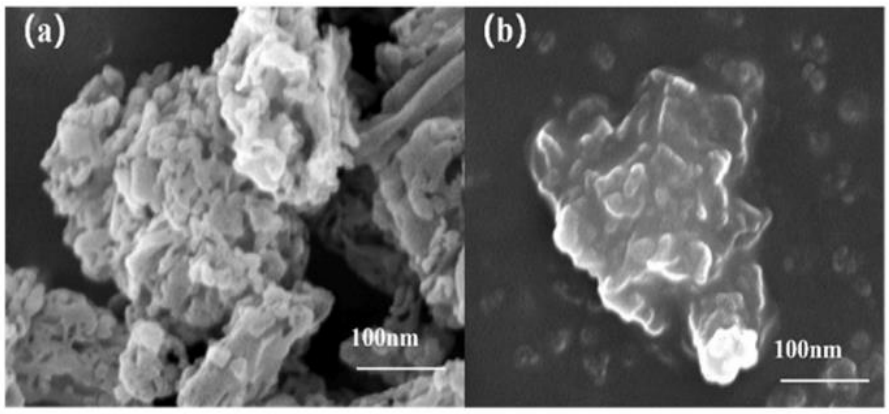

Figure 14. SEM images of, a) pure $mSiO_2$, b) PDMS/$mSiO_2$ particles.[172]

This is the accepted manuscript (postprint) of the following article:
Nazari, A., & Eslami-Farsani, R. (2025). A review of photothermal and superhydrophobic polymer nanocomposites as anti-icing nanocoatings. *Polymer Composites*, *46*(6), 5018-5040.
https://doi.org/10.1002/pc.29305

Liu et al,[173] joined a hybrid composite of TiO_2 nanobits and MWCNTs, referred to as TiO_2-MWCNTs, into an epoxy. This hybrid composite was then spray-coated onto a substratum and cured, causing a superhydrophobic skin characterized by superior abrasion resistance and de-icing efficiency. By varying the mass ratio of TiO_2 to MWCNTs, they discovered that a 3:1 ratio produced a WCA of 159.8º ± 0.5º. The integration of the TiO_2-MWCNTs not only enhanced the mechanical persistence of the veneer's surface but also utilized the exceptional photothermal transfortmation capabilities of the CNTs, thereby providing superior de-icing effectiveness to the coated surface. Figure 15 illustrates the Preparation schedule of TiO_2-MWCNTs.

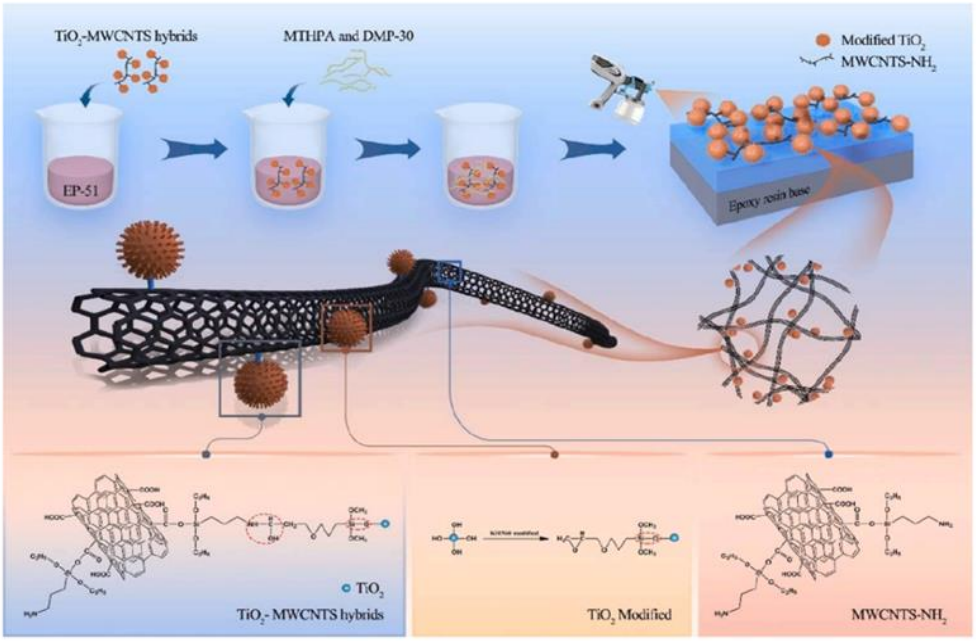

Figure 15. Preparation schedule of TiO_2-MWCNTs.[173]

Huang et al,[174] explored a newfound anti-icing/de-icing substance utilizing graphene foams (GF), which provided multiple functionalities, containing electrothermal, photothermal, and superhydrophobicity properties. The GF layer served as a bottom layer adhered to the substrate, while a polymer composite veneer loaded with TiN and SiO_2 nanoparticles was applied on top (Figure 16-a). This double-layered material, comprising the GF bottom lamella and the polymer composite veneer, was referred to as a graphene foam polymer composite (GFPC). As depicted in Figure 16(b), ice droplets could quickly melt and be removed through the combined effect of electric voltage and sunlight during the day or solely via an electric field at night. Remarkably, it was found that only a 1 V electric field was required to raise the face temperature from -10 °C to 1 °C within 400 seconds, which is significantly lower than previous materials that needed over 10 V to gain the same melting effect. Increasing the applied voltage slightly to 1.5 V resulted in a dramatic temperature augment from room temperature to over 150 °C within 200 seconds, versus to available electric heating methods that typically reach

This is the accepted manuscript (postprint) of the following article:
Nazari, A., & Eslami-Farsani, R. (2025). A review of photothermal and superhydrophobic polymer nanocomposites as anti-icing nanocoatings. *Polymer Composites*, *46*(6), 5018-5040.
https://doi.org/10.1002/pc.29305

peak temperatures of around 100 °C at much higher voltages. This exceptional performance allowed the GF-based substance to attain an impressive electrothermal energy transformation rate exceeding 90%. Moreover, the combination of sun irradiation and electricity not only reduced the minimum voltage needed to avoid ice formation but also enabled a much faster and more effective elimination of ice compared to using either electric or light fields alone.

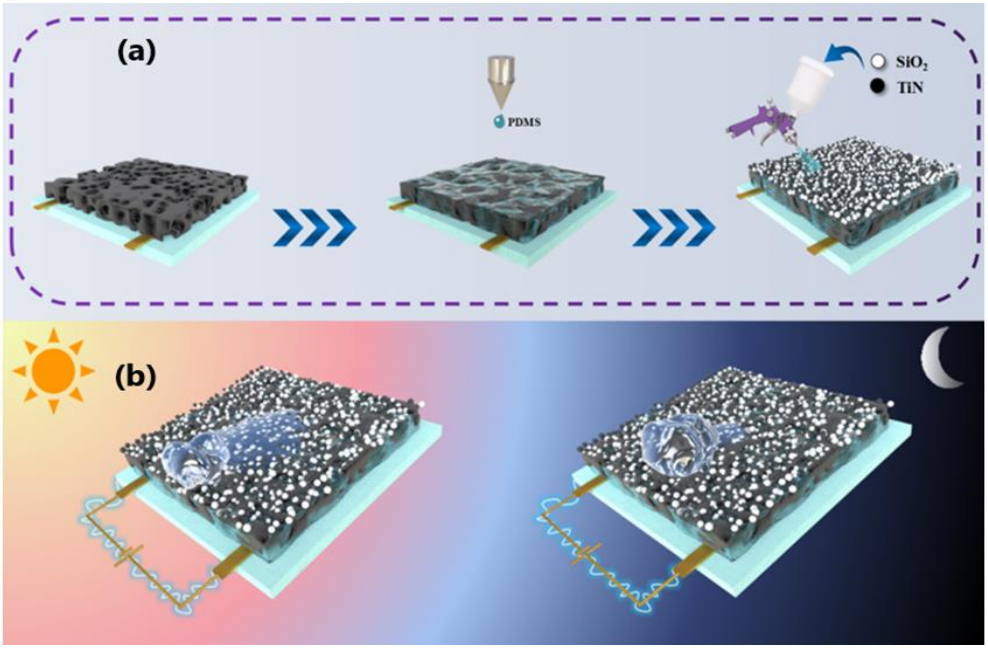

Figure 16. Schematics of, a) fabrication process of the GFPC, b) co-action of electric voltage and sunlight to melt and remove ice from GFPC surface.[174]

In another study, Chen et al,[175] developed a considerably effective photothermal superhydrophobic PDMS/Ni@Ti_3C_2Tx nanocomposite shield prepared cost-effectively. PDMS acted as a hydrophobic agent, sticky, and face preserver in this shield, while Ni@Ti_3C_2Tx served as an innovative magnetic photothermal additive. The resulting film, produced through this process, was named m-NMPA. Using a plain spraying technique, the additive was arranged by a drastic magnetic field to self-assemble into an eyelash-like microstructure order. This inimitable structure gave the surface superhydrophobic characteristics and formed an effective "light-capturing" system. Notably, the m-NMPA veneer exhibited exceptional superhydrophobic passive anti-icing and effective photothermal active de-icing capabilities. The micro/nano-structure of the veneer created a hollow section, meaningfully prolonging the icing time of water. Specifically, in extremely cold circumstances (-30 °C), the icing time was increased by a factor of 7.3 relative to the pristine substratum. Additionally, beneath sun irradiation, face droplets remained unfrozen. The outstanding photothermal efficiency was due to the tenacious anchoring of nickel bits on the MXene, enabling impressive photothermal synergy. The eyelash-like micro arrangement order also improved light-capturing efficiency, causing a high light absorption rate of 98%.

This is the accepted manuscript (postprint) of the following article:
Nazari, A., & Eslami-Farsani, R. (2025). A review of photothermal and superhydrophobic polymer nanocomposites as anti-icing nanocoatings. *Polymer Composites*, *46*(6), 5018-5040.
https://doi.org/10.1002/pc.29305

Ni@Ti_3C_2Tx hybrids were synthesized through a mild co-solvothermal method (Figure 17). Specifically, 1 g of Ti_3C_2Tx MXene nanosheets was dispersed in a mixture containing 80 mL of ethylene glycol (EG). Then, 4.05 g of $NiCl_2 \cdot 6H_2O$ was added to the suspension and agitated for 10 minutes. The pH of the blend was trimmed to approximately 11 using a 1 mol/L NaOH solution. Following this, 8.8 mL of $N_2H_4 \cdot H_2O$ was introduced and stirred to ensure all components were fully dissolved. The blend was then heated to 80 °C in an oil bath for 1 hour. After synthesis, the product was completely rinsed with water and alcohol before evaporating. Moreover, the microstructure helped retain heat at the surface's uppermost layer, optimizing heat energy utilization for melting and thawing ice. Beneath sunlight, the m-NMPA veneer could quickly fuse about a 4 mm thick ice pad in 558 seconds and eject the fused water immediately, minimizing the hazard of peripheral freezing. Moreover, the ice sticking force on the m-NMPA veneer's surface was notably low, with an adherence strength of nearly 4.7 kPa for a 1×1 cm^2 ice column. After doing extensive longevity trials containing xenon lamp weathering, pressure persistence, consecutive adhesive tape tests, xenon lamp exposure, water drop impact tests, and consecutive scrubbing with hydrochloric acid and bits, the layer maintained exceptional surface structure and superhydrophobic proficiency. The photothermal superhydrophobic passive anti-icing and active de-icing technologies presented in this research utilized tolerable solar energy for impressive thermal production. This approach offers a substantial potential for factual usages, boasting advantages such as plain manufacturing, environmental kindliness, excellent anti-freezing results, and remarkable persistence.

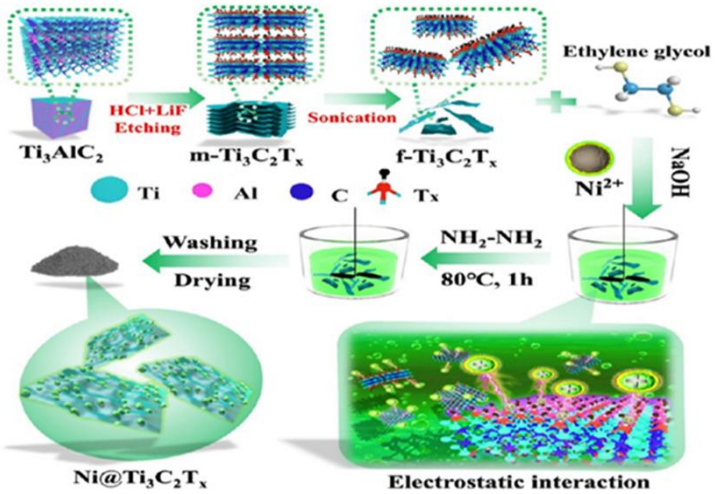

Figure 17. Schematic of the synthesis method and formation mechanism of Ni@Ti_3C_2Tx hybrids.[175]

4. Advantages and disadvantages of anti-icing and de-icing methods

In this research, various methods of dealing with the phenomenon of icing, which include active and passive de-icing, and active and passive anti-icing, were investigated. Each of these

This is the accepted manuscript (postprint) of the following article:
Nazari, A., & Eslami-Farsani, R. (2025). A review of photothermal and superhydrophobic polymer nanocomposites as anti-icing nanocoatings. *Polymer Composites*, *46*(6), 5018-5040.
https://doi.org/10.1002/pc.29305

methods has advantages and disadvantages. The advantages and disadvantages of the most commonly used methods are presented in Table 1.[12,14,34,176]

Table 1. The advantages and disadvantages of conventional anti-icing and de-icing methods

Anti-Icing and de-icing technology	**Advantage**	**Disadvantage**
Mechanical de-icing technology	Effective de-icing and easy removal of thick ice	High machine cost, waste of manpower, easy to damage surface
Heating de-icing and anti-icing Technology	The clear de-icing effect, short de-icing time, the wide application range	High energy consumption, easy to start a fire
Chemical-based de-icing and anti-icing technology	Lower the melting point of ice and completely remove the ice layer	Pollute the environment and corrode material surfaces
Superhydrophobic anti-icing nanocoating	Resource-saving, low-cost, and anti-icing effect	Poor mechanical stability
Photothermal de-icing nanocoating	Resource-saving, low-cost, and anti-icing effect	Poor mechanical stability and requires the presence of light

5. Perspective and summary

Many efforts and research have been made to deal with the phenomenon of icing. On the one hand, de-icing methods such as hot air flow, electrical current, and mechanical operations, and on the other hand, anti-icing methods such as surface super-hydrophobicity and the use of nanocoating have been performed. Because of the drawbacks and limitations related to de-icing methods, anti-icing methods are getting more attention nowadays.

Meanwhile, the use of polymer nanocomposites as a nanocoating has achieved very favorable results in the field of anti-icing procedures. These nanocoatings create anti-icing surfaces by making harshness on the surface and making the surface super-hydrophobic. The trend diagram with the topic of "polymer nanocomposite for anti-icing coatings" on Web of Science is shown in Figure 18.

This is the accepted manuscript (postprint) of the following article:
Nazari, A., & Eslami-Farsani, R. (2025). A review of photothermal and superhydrophobic polymer nanocomposites as anti-icing nanocoatings. *Polymer Composites*, *46*(6), 5018-5040.
https://doi.org/10.1002/pc.29305

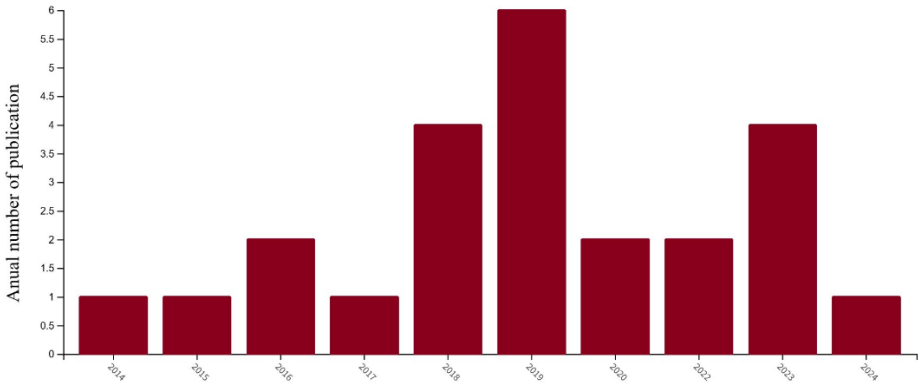

Figure 18. The number of published articles per year indexed in the Web of Science on the topic of "polymer nanocomposite for anti-icing coatings".

On the other hand, it should be noted that different procedures should be used to reach a complete anti-icing surface. Therefore, photothermal nanocomposites can be a suitable option in this regard. Because, at the same time that this group of polymer nanocomposites have superhydrophobic properties, they also generate heat when they are exposed to sunlight, which causes the ice to disappear and reduce its adhesion to the surface. The best nanoparticles to use in photothermal polymer nanocomposites are carbon nanoparticles and MXenes. This selection is due to the unique thermal and electrical properties of this group of nanoparticles. The trend diagram with the topic of "superhydrophobic and photothermal anti-icing nanocoating" on the Google Trends site is shown in Figure 19. As it is clear in the graph, in 2019 and 2022 a total of 182 articles with titles related to "superhydrophobic and photothermal anti-icing nanocoating" topics have been published, which shows the special characteristics of these nanocomposites as anti-icing nanocoatings.

On the other hand, polymer materials used in polymer nanocomposites can have unique properties, such as self-healing, apart from having hydrophobic properties. This issue increases the durability of this type of nanocoating. Silicone and PDMS polymer materials can be suitable options considering their characteristics in this regard.

This is the accepted manuscript (postprint) of the following article:
Nazari, A., & Eslami-Farsani, R. (2025). A review of photothermal and superhydrophobic polymer nanocomposites as anti-icing nanocoatings. *Polymer Composites*, *46*(6), 5018-5040.
https://doi.org/10.1002/pc.29305

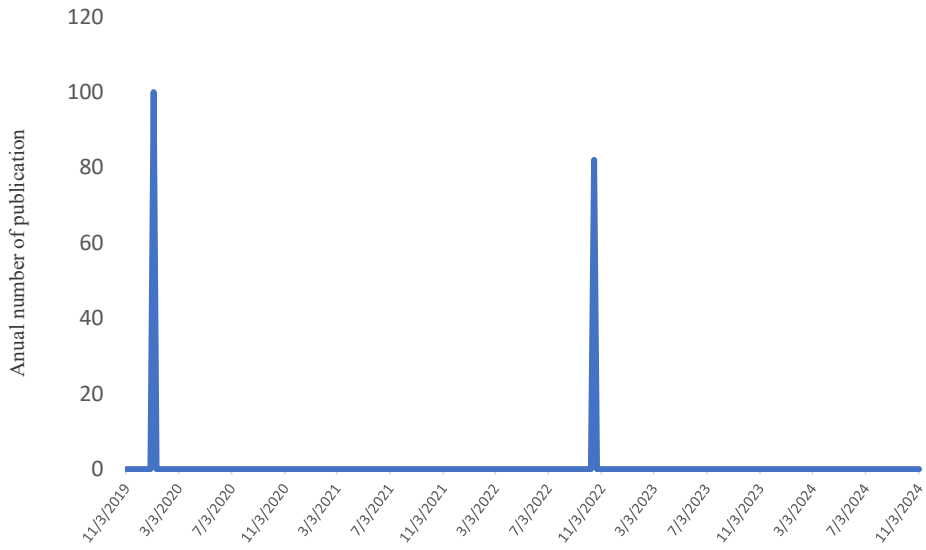

Figure 19. The number of published articles per year indexed in the Google Trends site on the topic of "superhydrophobe and photothermal anti-icing nanocoating".

6. Conclusion

In this research, types of ice have been explored in terms of their appearance and how they are formed. Also, various theories of wetting and icing mechanisms have been analyzed. At last, the types of methods to counteract icing, such as surface superhydrophobicity and anti-icing nanocoatings, have been investigated. Organic and inorganic nanomaterials, mainly SiO_2, CNTs, graphene, carbon nanofibers, CuO, Fe_3O_4, TiO_2, TiN, and MXenes can be incorporated to develop anti-icing polymer nanocomposites. Polymer matrixes, especially PMMA, PDMS, PTFE, silicone, and polyurethane can be incorporated to develop anti-icing polymer nanocomposites. Superhydrophobic polymer nanocomposite veneers developed by joining the area of polymer composite technology, nanoscience, and superhydrophobicity have emerged as an impressive way to ameliorate anti-icing veneer characteristics. Photothermal polymer nanocomposites are established on conventional superhydrophobic surfaces to add photothermal substances for amendment, which photothermal substances have a high sunlight absorption level, and do not affect the primary properties of the veneer.

References

1. Bartels-Rausch T. Ten things we need to know about ice and snow. *Nature*. 2013; 494 (7435):27-29. DOI: 10.1038/494027a.

2. Andrey J. Long-term trends in weather-related crash risks. *Journal of Transport Geography*. 2010; 18 (2): 247-258. doi: 10.1016/j.jtrangeo.2009.05.002.

3. Thomas SK, Cassoni RP, MacArthur CD. Aircraft anti-icing and de-icing techniques and modeling. *Journal of Aircraft.* 1996; 33 (5): 841-854. doi: 10.2514/3.47027.

4. Parent O, Ilinca A. Anti-icing and de-icing techniques for wind turbines: Critical review. *Cold Regions Science and Technology*. 2011; 65 (1): 88-96. doi: 10.1016/j.coldregions.2010.01.005.

5. Hu YZ, Yu SF, Zhang L, Liu P. Research and validation on melting ice of overhead transmission line. *Applied Mechanics and Materials.* 2014; 543: 653-657. doi: 10.4028/www.scientific.net/amm.543-547.653.

6. Liu Y, Yang W, Liu Y, Xu R, Liu S, Zhou F. Robust photothermal coating strategy for efficient ice removal. *ACS Applied Materials & Interfaces*. 2020; 12(41): 46981-46990. doi: 10.1021/acsami.0c13367.

7. Kleissl K, Georgakis C. Bridge ice accretion and de-and anti-icing systems: A review. In *The 7th international cable supported bridge operators' conference 2010***,** Jiangsu, China. 2010; pp 161-167.

8. Ryerson CC. Assessment of Superstructure Ice Protection as Applied to Offshore Oil Operations Safety. *US Army Research*. 2009; pp 49.

9. Makkonen L. Ice adhesion—theory, measurements and countermeasures. *Journal of Adhesion Science and Technology*. 2012; 26(4-5): 413-445. doi: 10.1163/016942411X574583.

10. Müller NC, Hansen BL, Borup KT, Hann R. Development of an ice protection system for the propeller of a small UAV. *Cold Regions Science and Technology*. 2023; 213: 103938. doi: 10.1016/j.coldregions.2023.103938.

11. Zhou L, Yi X, Liu Q. A Review of Icing Research and Development of Icing Mitigation Techniques for Fixed-Wing UAVs. *Drones.* 2023; 7(12): 709. doi: 10.3390/drones7120709.

12. Cornell JS, Pillard DA, Hernandez MT. Comparative measures of the toxicity of component chemicals in aircraft deicing fluid. *Environmental Toxicology and Chemistry: An International Journal.* 2000; 19(6): 1465-1472. doi: 10.1002/etc.5620190601.

13. Ramakrishna DM, Viraraghavan T. Environmental impact of chemical deicers–a review. *Water, Air, and Soil Pollution.* 2005; 166: 49-63. doi: 10.1007/s11270-005-8265-9.

14. Fay, L.; Shi, X. Environmental impacts of chemicals for snow and ice control: state of the knowledge. *Water, Air, & Soil Pollution.* 2012; 223: 2751-2770. doi: 10.1007/s11270-011-1064-6.

15. Charpentier TVJ, Neville A, Millner P, Hewson R, Morina A. An investigation of freezing of supercooled water on anti-freeze protein modified surfaces. *Journal of Bionic Engineering.* 2013; 10(2): 139-147. doi: 10.1016/S1672-6529(13)60208-5.

16. Chenxi Z, Jilan L, Lingdong C, et al. Dark, heat-reflective, anti-ice rain and superhydrophobic cement concrete surfaces. *Construction and Building Materials.* 2019; 220: 21-28. doi: 10.1016/j.conbuildmat.2019.05.188.

17. Subramanyam SB, Kondrashov V, Rühe J, Varnasi KK. Low ice adhesion on nano-textured superhydrophobic surfaces under supersaturated conditions. *ACS Applied Materials & Interfaces.* 2016; 8(20): 12583-12587. doi: 10.1021/acsami.6b01133.

18. Coclite AM, Howden MR, Borrelli DC. 25th anniversary article; CVD polymers: a new paradigm for surface modifi cation and device fabrication. *Advanced Materials.* 2013; 25(38): 5392-5423. doi: 10.1002/adma.201301878.

19. Golovin K, Kobaku SPR, Lee DH, Diloreto ET, Mabry JM, Tuteja A. Designing durable icephobic surfaces. *Science Advances.* 2016; 2(3): e1501496. doi: 10.1126/sciadv.1501496.

20. Farzaneh M, Jakl F, Arabani MP, et al. Systems for Prediction and Monitoring of Ice Shedding, Anti-icing and De-icing for power line conductors and ground wires. *CIGRE, working paper.* 2010; pp 9-15.

21. Leblond A, Sugawara N, Asano Y, Isozaki M. New results on the anti-icing performance of lc-spiral rods. *The 14th International Workshop on Atmospheric Icing of Structures 2011,* Chongqing, China. 2011; pp 1-5.

22. Piscitelli F, Palazzo S, Nicola FD. Icing Wind Tunnel Test Campaign on a Nacelle Lip-Skin to Assess the Effect of a Superhydrophobic Coating on Ice Accretion. *Applied Sciences.* 2023; 13(8): 5183. doi: 10.3390/app13085183

23. Wang M, Gao H, Chai M, Sun Z, Wang J. Study on the Performances of an Anticoagulant Ice Coating Material for Asphalt Pavement. In *Journal of Physics: Conference Series*. 2022; Vol. 2168. No. 1, 012014.

24. Dong W, Zhu J, Zheng M, Chen Y. Thermal analysis and testing of nonrotating cone with hot-air anti-icing system. *Journal of Propulsion and Power.* 2015; 31(3): 896-903. doi: 10.2514/1. B35378.

25. Boinovich LB, Emelyanenko AM. Anti-icing potential of superhydrophobic coatings. *Mendeleev Communications.* 2013, 1(23): 3-10. doi: 10.1016%2Fj.mencom.2013.01.002.

26. Masoud F, Charles RC. Anti-icing and deicing techniques. *Cold Regions Science and Technology.* 2011; 65(1): 1-4. doi: 10.1016/j.coldregions.2010.08.012.

27. Hasan A, Eslami-Farsani R, Ebrahimnezhad-Khaljiri H. Effect of ZrO_2 nanoparticles on the self-lubrication behavior of the linseed oil-loaded microcapsule/epoxy composite coatings. *Ceramics International*. 2024; 50(19): 36544-36554. https://doi.org/10.1016/j.ceramint.2024.07.039.

28. Jalali H, Eslami-Farsani R, Ramezanzadeh B. Designing a smart epoxy anti-corrosion coating loaded with molybdate-doped polythiophene nano-hybrid self-assembled multi-walled carbon nanotube. *Progress in Organic Coatings*. 2024; 188: 108217. https://doi.org/10.1016/j.porgcoat.2024.108217.

29. Nazari A. An experimental investigation on the flexural and wear properties of multiscale nanoclay/basalt fiber/epoxy composites. *Polymer Composites.* 2021; 42(11): 5755-5762. doi: 10.1002/pc.26257.

30. Jalali H, Eslami-Farsani R, Ramezanzadeh B. Molybdate-doped sulfonated-polyaniline (SPni. Mo) grafted CNT nano-particles for fabrication of a dual-functional epoxy composite coating with durable corrosion resistance function. *Colloids and Surfaces A: Physicochemical and Engineering Aspects*. 2023; 677: 132433. https://doi.org/10.1016/j.colsurfa.2023.132433.

31. Kazemi-Khasragh E, Bahari-sambran F, Platzer C, Eslami-Farsani R. The synergistic effect of graphene nanoplatelets–montmorillonite hybrid system on tribological behavior of epoxy-based nanocomposites. *Tribology International.* 2020; 151: 106472. doi: 10.1016/j.triboint.2020.106472.

32. Eslami-Farsani R, Daghigh V, Derakhshani K. Tensile and flexural properties of basalt fibers/nano-alumina powder-reinforced multi-scale composites. *Surfaces and Interfaces.* 2024; 46: 104009. doi: 10.1016/j.surfin.2024.104009.

33. Wang F, Tay TE, Sun Y, Liang W, Yang B. Low-voltage and-surface energy SWCNT/poly (dimethylsiloxane)(PDMS) nanocomposite film: Surface wettability for passive anti-icing and surface-skin heating for active deicing. *Composites science and technology*. 2019; 184: 107872. doi: 10.1016/j.compscitech.2019.107872.

34. Vafaeenezhad H, Eslami-Farsani R. Self-Healing and Self-Lubricating Nano-hybrid Smart Coatings. *Nano-hybrid Smart Coatings: Advancements in Industrial Efficiency and Corrosion Resistance. American Chemical Society*. 2024; 303-352. doi: 10.1021/bk-2024-1469.ch014.

35. Liu X, Chen H, Kou W, Zhang D. Robust anti-icing coatings via enhanced superhydrophobicity on fiberglass cloth. *Cold Regions Science and Technology.* 2017; 138: 18-23. doi: 10.1016/j.coldregions.2017.03.004.

36. Zeng D, Li Y, Huan D, et al. Robust epoxy-modified superhydrophobic coating for aircraft anti-icing systems. *Colloids and Surfaces A: Physicochemical and Engineering Aspects.* 2021; 628: 127377. doi: 10.1016/j.colsurfa.2021.127377.

37. Gao F, Song L, Tong Z, et al. A robust and multi-functional nanocomposite with "soft and hard" nanodomains against harsh environments. *Chemical Engineering Journal.* 2023; 455: 139894. doi: 10.1016/j.cej.2022.139894.

38. Ghorbani M, Ebrahimnezhad-Khaljiri H, Eslami-Farsani R, Vafaeenezhad H. The synergic effect of microcapsules and titanium nanoparticles on the self-healing and self-lubricating epoxy coatings: A dual smart application. *Surfaces and Interfaces*. 2021; 23: 100998. https://doi.org/10.1016/j.surfin.2021.100998.

39. Wang F, Guo F, Tang M, Zhang X, Zhang Z, Li S, Yang B. 3-D computational study of a single droplet impacting the random rough surface: Hydromechanical solidification. *International Journal of Heat and Mass Transfer*. 2024; 224: 125311. doi: 10.1016/j.ijheatmasstransfer.2024.125311.

40. Solangi AR. Icing effects on power lines and anti-icing and de-icing methods. MS. Dissertation, UiT the Arctic University, Norway. 2018. https://hdl.handle.net/10037/14198.

41. Merrill HM, Feltes JW. Transmission icing: a physical risk with a physical hedge. In *Power Engineering Society General Meeting 2006*, *IEEE*, Montreal, Canada. 2006; pp 7-pp. doi: 10.1109/PES.2006.1709619.

42. Barabadi A, Garmabaki AHS, Zaki R. Designing for performability: An icing risk index for Arctic offshore. *Cold Regions Science and Technology.* 2016; 124: 77-86. doi: 10.1016/j.coldregions.2015.12.013.

43. Heyun L, Xiaosong G, Wenbin T. Icing and anti-icing of railway contact wires. In *Reliability and safety in railway, IntechOpen*. 2012; pp 295-316.

44. Dyke PV, Havard DG. Effect of ice and snow on the dynamics of transmission line cables, part I: Aeolian vibration, wake-induced oscillation and galloping motions. In *Proceedings of the 11 International Workshop Atmospheric Icing of Structure 2005,* Montreal, Canada. 2005; pp 285-290.

45. Šabata J, Lehký P, Zeman L, Vaculík P. Automated Icing Monitoring System on the territory of the Czech and Slovak Republic. In *16th international workshop on atmospheric icing of structures, IWAIS.* 2015.

46. Huang X, Tepylo N, Pommier-Budinger V, Budinger M, Bonaccurso E, Villedieu P, Bennani L. A survey of icephobic coatings and their potential use in a hybrid coating/active ice protection system for aerospace applications. *Progress in Aerospace Sciences*. 2019; 105: 74-97. doi: 10.1016/j.paerosci.2019.01.002.

47. Zhang Z, Liu XY. Control of ice nucleation: freezing and antifreeze strategies. *Chemical Society Reviews*. 2018; 47(18): 7116-7139. doi: 10.1039/C8CS00626A.

48. Wang F, Sun Y, Liang W, He H, Yang B, Bonsu AO. The three-line synergistic icephobicity of conductive CNTs/PDMS nanocomposite with bio-inspired hierarchical surface. *Surfaces and Interfaces*. 2021; 26: 101424. doi: 10.1016/j.surfin.2021.101424.

49. Jiaqiang E, Jin Y, Deng Y, et al. Wetting models and working mechanisms of typical surfaces existing in nature and their application on superhydrophobic surfaces: A review. *Adv. Mater. Interfaces*. 2018; 5: 1701052. doi: 10.1002/admi.201701052.

50. Borgioli F, Galvanetto E, Bacci T. Influence of surface morphology and roughness on water wetting properties of low temperature nitrided austenitic stainless steels. *Materials Characterization*. 2004; 95: 278-284. doi: 10.1016/j.matchar.2014.07.006.

51. Feng L, Li S, Li Y, et al. Super-hydrophobic surfaces: from natural to artificial. *Advanced Materials*. 2002; 14(24): 1857-1860. doi: 10.1002/adma.200290020.

52. Parvate S, Dixit P, Chattopadhyay S. Superhydrophobic surfaces: insights from theory and experiment. *The Journal of Physical Chemistry B*. 2020; 124(8): 1323-1360. doi: 10.1021/acs.jpcb.9b08567.

53. Kreder MJ, Alvarenga J, Kim P, Aizenberg J. Design of anti-icing surfaces: smooth, textured or slippery?. *Nature Reviews Materials*. 2016; 1(1): 1-15. doi: 10.1038/natrevmats.2015.3.

54. Kumar V, Verma R, Sharma VS, Sharma V. Recent progresses in super-hydrophobicity and micro-texturing for engineering applications. *Surface Topography: Metrology and Properties*. 2022; 9(4): 043003. doi: 10.1088/2051-672X/ac4321.

55. Young T. III. An essay on the cohesion of fluids. *Philosophical Transactions of the Royal Society of London*. 1805; (95): 65-87. doi: 10.1098/rstl.1805.0005.

56. Li W, Zhan Y, Yu S. Applications of superhydrophobic coatings in anti-icing: Theory, mechanisms, impact factors, challenges and perspectives. *Progress in Organic Coatings*. 2021; 152: 106117. doi: 10.1016/j.porgcoat.2020.106117.

57. Wenzel RN. Resistance of solid surfaces to wetting by water. *Industrial & Engineering Chemistry*. 1936; 28(8): 988-994. doi: 10.1021/ie50320a024.

58. Cassie ABD, Baxter S. Wettability of porous surfaces. *Transactions of the Faraday Society*. 1944; 40: 546-551. doi: 10.1039/TF9444000546.

59. Furmidge CGL. Studies at phase interfaces. I. The sliding of liquid drops on solid surfaces and a theory for spray retention. *Journal of Colloid Science*. 1962; 17(4): 309-324. doi: 10.1016/0095-8522(62)90011-9.

60. Bayat A, Ebrahimi M, Ardekani SR, Iranizad ES, Moshfegh AZ. Extended Gibbs free energy and laplace pressure of ordered hexagonal close-packed spherical particles: A wettability study. *Langmuir*. 2021; 37(28): 8382-8392. doi: 10.1021/acs.langmuir.1c00343.

61. Marmur A. Wetting on hydrophobic rough surfaces: to be heterogeneous or not to be?. *Langmuir*. 2003; 19(20): 8343-8348. doi: 10.1021/la0344682.

62. Varanasi KK, Hsu M, Bhate N, Yang W, Deng T. Spatial control in the heterogeneous nucleation of water. *Applied Physics Letters*. 2009; 95(9): doi: 10.1063/1.3200951.

63. Sigsbee RA. Adatom capture and growth rates of nuclei. *Journal of Applied Physics*. 1971; 42(10): 3904-3915. doi: 10.1063/1.1659705.

64. Wilson CTR. IX. On the condensation nuclei produced in gases by the action of Röntgen rays. Uranium rays, ultra-violet light, and other agents. *Philosophical Transactions of the Royal Society of London*, *Series A, Containing Papers of a Mathematical or Physical Character*. 1899; 192: 403-453. doi: 10.1098/rsta.1899.0009.

65. Skinner LM, Sambles JR. The Kelvin equation-a review. *Journal of Aerosol Science*. 1972; 3(3): 199-210. doi: 10.1016/0021-8502(72)90158-9.

66. Liu XY. Heterogeneous nucleation or homogeneous nucleation? The Journal of Chemical Physics. 2000; 112(22): 9949-9955. doi: 10.1063/1.481644.

67. Irajizad P, Nazifi S, Ghasemi H. Icephobic surfaces: Definition and figures of merit. *Advances in Colloid and Interface Science*. 2019; 269: 203-218. doi: 10.1016/j.cis.2019.04.005.

68. Pruppacher HR, Klett JD. Microstructure of Atmospheric Clouds and Precipitation. In *Microphysics of Clouds and Precipitation, Springer*. 2010; pp 10-73.

69. Yancheshme AA, Momen G, Aminabadi RJ. Mechanisms of ice formation and propagation on superhydrophobic surfaces: A review. *Advances in Colloid and Interface Science*. 2020; 279: 102155. doi: 10.1016/j.cis.2020.102155.

70. Zhang H, Guo H, Jiang R, Wan W, Deng P, Zhou X. Research progress of multifunctional anti-icing composites materials. *Journal of Applied Polymer Science*. 2024; 141(36): e55922. doi: 10.1002/app.55922.

71. Jamil MI, Ali A, Haq F, Zhang Q, Zhan X, Chen F. Icephobic strategies and materials with superwettability: design principles and mechanism. *Langmuir*. 2018; 34(50): 15425-15444. doi: 10.1021/acs.langmuir.8b03276.

72. Schutzius TM, Jung S, Maitra T, et al. Physics of icing and rational design of surfaces with extraordinary icephobicity. *Langmuir*. 2015; 31(17): 4807-4821. doi: 10.1021/la502586a.

73. Ladino-Moreno LA, Stetzer O, Lohmann U. Contact freezing: a review of experimental studies. *Atmospheric Chemistry and Physics*. 2013; 13(19): 9745-9769. doi: 10.5194/acp-13-9745-2013.

74. Gohari B, Russell K, Hejazi V, Rohatgi P. Role of water solidification concepts in designing nano-textured anti-icing surfaces. *The Journal of Physical Chemistry B*. 2017; 121(32): 7527-7535. doi: 10.1021/acs.jpcb.7b04081.

75. Amirfazli A, Antonini C. Fundamentals of anti-Icing surfaces. In *Non-wettable Surfaces: Theory, Preparation, and Applications, The Royal Society of Chemistry*. 2016; pp 319-346. doi: 10.1039/9781782623953-00319.

76. Gao J, Martin A, Yatvin J, White E, Locklin, J. Permanently grafted icephobic nanocomposites with high abrasion resistance. *Journal of Materials Chemistry A*. 2016; 4(30): 11719-11728. doi: 10.1039/C6TA03222B.

77. Li XM, Reinhoudt D, Crego-Calama M. What do we need for a superhydrophobic surface? A review on the recent progress in the preparation of superhydrophobic surfaces. *Chemical Society Reviews*. 2007; 36(8): 1350-1368. doi: 10.1039/B602486F.

78. Li J, Fu J, Cong Y, Wu Y, Xue L, Han Y. Macroporous fluoropolymeric films templated by silica colloidal assembly: A possible route to super-hydrophobic surfaces. *Applied Surface Science*. 2006; 252(6): 2229-2234. doi: 10.1016/j.apsusc.2005.03.224.

79. Stelmashuk V, Biederman H, Slavinska D, Zemek J, Trchova M. Plasma polymer films rf sputtered from PTFE under various argon pressures. *Vacuum*. 2005; 77(2): 131-137. doi: 10.1016/j.vacuum.2004.08.011.

80. Kim SH, Kim JH, Kang BK, Uhm HS. Superhydrophobic CF_x coating via in-line atmospheric RF plasma of He-CF4-H2. *Langmuir*. 2005; 21(26): 12213-12217. doi: 10.1021/la0521948.

81. Carpentier J, Grundmeier G. Chemical structure and morphology of thin bilayer and composite organosilicon and fluorocarbon microwave plasma polymer films. *Surface and Coatings Technology*. 2005; 192(2-3): 189-198. doi: 10.1016/j.surfcoat.2004.05.019.

82. Fresnais J, Benyahia L, Poncin-Epaillard F. Dynamic (de) wetting properties of superhydrophobic plasma-treated polyethylene surfaces. *Surface and Interface Analysis*. 2006; 38(3): 144-149. doi: 10.1002/sia.2235.

83. Kiuru M, Alakoski E. Low sliding angles in hydrophobic and oleophobic coatings prepared with plasma discharge method. *Materials Letters*. 2004; 58(16): 2213-2216. doi: 10.1016/j.matlet.2004.01.024.

84. Lee SJ, Paik BG, Kim GB, Jang YG. Self-cleaning features of plasma-treated surfaces with self-assembled monolayer coating. *Japanese Journal of Applied Physics*. 2006; 45(2R): 912. doi: 10.1143/JJAP.45.912.

85. Liang J, Liu BQ. Intromission of water-repellent and hydroscopic properties simultaneously to PP by plasma discharge method. *Chinese Journal of Polymer Science*. 2005; 23(01): 83-92.

86. Teare DOH, Spanos CG, Ridley P, et al. Pulsed plasma deposition of super-hydrophobic nanospheres. *Chemistry of Materials*. 2002; 14(11): 4566-4571. doi: 10.1021/cm011600f.

87. Teshima K, Sugimura H, Inoue Y, Takai O, Takano A. Transparent ultra water-repellent poly (ethylene terephthalate) substrates fabricated by oxygen plasma treatment and subsequent hydrophobic coating. *Applied Surface Science*. 2005; 244(1-4): 619-622. doi: 10.1016/j.apsusc.2004.10.143.

88. Teshima K, Sugimura H, Inoue Y, Takai O, Takano A. Wettability of Poly (ethylene terephthalate) Substrates Modified by a Two-Step Plasma Process: Ultra Water Repellent Surface Fabrication. *Chemical Vapor Deposition*. 2004; 10(6): 295-297. doi: 10.1002/cvde.200304181.

89. Wu Y, Bekke M, Inoue Y, et al. Mechanical durability of ultra-water-repellent thin film by microwave plasma-enhanced CVD. *Thin Solid Films*. 2004; 457(1): 122-127. doi: 10.1016/j.tsf.2003.12.007.

90. Han JT, Zheng Y, Cho JH, Xu X, Cho K. Stable superhydrophobic organic-inorganic hybrid films by electrostatic self-assembly. *The Journal of Physical Chemistry B*. 2005; 109(44): 20773-20778. doi: 10.1021/jp052691x.

91. Li XM, Reinhoudt D, Crego-Calama M. What do we need for a superhydrophobic surface? A review on the recent progress in the preparation of superhydrophobic surfaces. *Chemical Society Reviews*. 2007; 36(8): 1350-1368. doi: 10.1039/B602486F.

92. Zhang Q, Xia F, Sun T, et al. Wettability switching between high hydrophilicity at low pH and high hydrophobicity at high pH on surface based on pH-responsive polymer. *Chemical Communications*. 2008; 10: 1199-1201. doi: 10.1039/B716681H.

93. Kulinich SA, Farzaneh M. Hydrophobic properties of surfaces coated with fluoroalkylsiloxane and alkylsiloxane monolayers. *Surface Science*. 2004; 573(3): 379-390. doi: 10.1016/j.susc.2004.10.008.

94. Schondelmaier D, Cramm S, Klingeler R, Morenzin J, Zilkens C, Eberhardt W. Orientation and self-assembly of hydrophobic fluoroalkylsilanes. *Langmuir*. 2002; 18(16): 6242-6245. doi: 10.1021/la0256533.

95. Soeno T, Inokuchi K, Shiratori S. Ultra-water-repellent surface: fabrication of complicated structure of SiO_2 nanoparticles by electrostatic self-assembled films. *Applied Surface Science*. 2004; 237(1-4): 539-543. doi: 10.1016/j.apsusc.2004.06.041.

96. Song X, Zhai J, Wang Y, Jiang L. Fabrication of superhydrophobic surfaces by self-assembly and their water-adhesion properties. *The Journal of Physical Chemistry B*. 2005; 109(9): 4048-4052. doi: 10.1021/jp045152l.

97. Zhang G, Wang D, Gu ZZ, Möhwald H. Fabrication of superhydrophobic surfaces from binary colloidal assembly. *Langmuir*. 2005; 21(20): 9143-9148. doi: 10.1021/la0511945.

98. Zhao N, Shi F, Wang Z, Zhang X. Combining layer-by-layer assembly with electrodeposition of silver aggregates for fabricating superhydrophobic surfaces. *Langmuir*. 2005; 21(10): 4713-4716. doi: 10.1021/la0469194.

99. Wu Y, Sugimura H, Inoue Y, Takai O. Thin films with nanotextures for transparent and ultra water-repellent coatings produced from trimethylmethoxysilane by microwave plasma CVD. *Chemical Vapor Deposition*. 2002; 8(2): 47-50. doi: 10.1002/1521-3862(20020304)8:2%3C47::AID-CVDE47%3E3.0.CO;2-%23.

100. Shi F, Wang Z, Zhang X. Combining a layer-by-layer assembling technique with electrochemical deposition of gold aggregates to mimic the legs of water striders. *Advanced Materials*. 2005; 17(8): 1005-1009. doi: 10.1002/adma.200402090.

101. Ma M, Mao Y, Gupta M, Gleason KK, Rutledge GC. Superhydrophobic fabrics produced by electrospinning and chemical vapor deposition. *Macromolecules*. 2005; 38(23): 9742-9748. doi: 10.1021/ma0511189.

102. Liu H, Feng L, Zhai J, Jiang L, Zhu D. Reversible wettability of a chemical vapor deposition prepared ZnO film between superhydrophobicity and superhydrophilicity. *Langmuir*. 2004; 20(14): 5659-5661. doi: 10.1021/la036280o.

103. Li M, Zhai J, Liu H, Song Y, Jiang L, Zhu D. Electrochemical deposition of conductive superhydrophobic zinc oxide thin films. *The Journal of Physical Chemistry B*. 2003; 107(37): 9954-9957. doi: 10.1021/jp035562u.

104. Hosono E, Fujihara S, Honma I, Zhou H. Superhydrophobic perpendicular nanopin film by the bottom-up process. *Journal of the American Chemical Society*. 2005; 127(39): 13458-13459. doi: 10.1021/ja053745j.

105. Han JT, Lee DH, Ryu CY, Cho K. Fabrication of superhydrophobic surface from a supramolecular organosilane with quadruple hydrogen bonding. *Journal of the American Chemical Society*. 2004; 126(15): 4796-4797. doi: 10.1021/ja0499400.

106. Hikita M, Tanaka K, Nakamura T, Kajiyama T, Takahara A. Super-liquid-repellent surfaces prepared by colloidal silica nanoparticles covered with fluoroalkyl groups. *Langmuir*. 2005; 21(16): 7299-7302. doi: 10.1021/la050901r.

107. Li XM, Reinhoudt D, Crego-Calama M. What do we need for a superhydrophobic surface? A review on the recent progress in the preparation of superhydrophobic surfaces. *Chemical Society Reviews*. 2007; 36(8): 1350-1368. doi: 10.1039/B602486F.

108. Li Y, Cai W, Cao B, Duan G, Sun F. Fabrication of the periodic nanopillar arrays by heat-induced deformation of 2D polymer colloidal monolayer. *Polymer*. 2005; 46(26): 12033-12036. doi: 10.1016/j.polymer.2005.10.112.

109. Nakajima A, Saiki C, Hashimoto K, Watanabe T. Processing of roughened silica film by coagulated colloidal silica for super-hydrophobic coating. *Journal of Materials Science Letters*. 2001; 20: 1975-1977. doi: 10.1023/A:1013199105688.

110. Jiang L, Zhao Y, Zhai J. A lotus-leaf-like superhydrophobic surface: a porous microsphere/nanofiber composite film prepared by electrohydrodynamics. *Angewandte Chemie-International Edition*. 2004; 43(33): 4338-4341. doi: 10.1002/anie.200460333.

111. Miyauchi Y, Ding B, Shiratori S. Fabrication of a silver-ragwort-leaf-like super-hydrophobic micro/nanoporous fibrous mat surface by electrospinning. *Nanotechnology*. 2006; 17(20): 5151. doi: 10.1088/0957-4484/17/20/019.

112. Singh A, Steely L, Allcock HR. Poly [bis (2, 2, 2-trifluoroethoxy) phosphazene] superhydrophobic nanofibers. *Langmuir*. 2005; 21(25): 11604-11607. doi: 10.1021/la052110v.

113. Acatay K, Simsek E, Ow-Yang C, Menceloglu YZ. Tunable, superhydrophobically stable polymeric surfaces by electrospinning. *Angewandte Chemie*. 2004; 116(39): 5322-5325. doi: 10.1002/ange.200461092.

114. Suh KY, Jon S. Control over wettability of polyethylene glycol surfaces using capillary lithography. *Langmuir*. 2005; 21(15): 6836-6841. doi: 10.1021/la050878+.

115. He B, Patankar NA, Lee J. Multiple equilibrium droplet shapes and design criterion for rough hydrophobic surfaces. *Langmuir*. 2003; 19(12): 4999-5003. doi: 10.1021/la0268348.

116. Fürstner R, Barthlott W, Neinhuis C, Walzel P. Wetting and self-cleaning properties of artificial superhydrophobic surfaces. *Langmuir*. 2005 ; 21(3) : 956-961. doi: 10.1021/la0401011

117. Öner D, McCarthy TJ. Ultrahydrophobic surfaces. Effects of topography length scales on wettability. *Langmuir*. 2000; 16(20): 7777-7782. doi: 10.1021/la000598o.

118. Patankar NA. Mimicking the lotus effect: influence of double roughness structures and slender pillars. *Langmuir*. 2004 ; 20(19) : 8209-8213. doi: 10.1021/la048629t.

119. Patankar NA. Transition between superhydrophobic states on rough surfaces. *Langmuir*. 2004; 20(17): 7097-7102. doi: 10.1021/la049329e.

120. Patankar NA. On the modeling of hydrophobic contact angles on rough surfaces. *Langmuir*. 2003; 19(4): 1249-1253. doi: 10.1021/la026612+.

121. Martines E, Seunarine K, Morgan H, Gadegaard N, Wilkinson CD, Riehle MO. Superhydrophobicity and superhydrophilicity of regular nanopatterns. *Nano Letters*. 2005; 5(10): 2097-2103. doi: 10.1021/nl051435t.

122. Yoshimitsu Z, Nakajima A, Watanabe T, Hashimoto K. Effects of surface structure on the hydrophobicity and sliding behavior of water droplets. *Langmuir*. 2002; 18(15): 5818-5822. doi: 10.1021/la020088p.

123. Jin M, Feng X, Feng L, et al. Superhydrophobic aligned polystyrene nanotube films with high adhesive force. *Advanced Materials*. 2005; 17(16): 1977-1981. doi: 10.1002/adma.200401726.

124. Nakajima A, Abe K, Hashimoto K, Watanabe T. Preparation of hard super-hydrophobic films with visible light transmission. *Thin Solid Films*. 2000; 376(1-2): 140-143. doi: 10.1016/S0040-6090(00)01417-6.

125. Nakajima A, Fujishima A, Hashimoto K, Watanabe T. Preparation of transparent superhydrophobic boehmite and silica films by sublimation of aluminum acetylacetonate. *Advanced Materials*. 1999; 11(16): 1365-1368. doi: 10.1002/(SICI)1521-4095(199911)11:16%3C1365::AID-ADMA1365%3E3.0.CO;2-F.

126. Minko S, Müller M, Motornov M, Nitschke M, Grundke K, Stamm M. Two-level structured self-adaptive surfaces with reversibly tunable properties. *Journal of the American Chemical Society*. 2003; 125(13): 3896-3900. doi: 10.1021/ja0279693.

127. Khorasani MT, Mirzadeh H. In vitro blood compatibility of modified PDMS surfaces as superhydrophobic and superhydrophilic materials. *Journal of Applied Polymer Science*. 2004; 91(3): 2042-2047. doi: 10.1002/app.13355.

128. Khorasani MT, Mirzadeh H, Kermani Z. Wettability of porous polydimethylsiloxane surface: morphology study. *Applied Surface Science*. 2005; 242(3-4): 339-345. doi: 10.1016/j.apsusc.2004.08.035.

129. Daoud WA, Xin JH, Tao X. Superhydrophobic silica nanocomposite coating by a low-temperature process. *Journal of the American Ceramic Society*. 2004; 87(9): 1782-1784. doi: 10.1111/j.1551-2916.2004. 01782.x.

130. Zhang X, Hillenbrand J, Sessler GM. Thermally stable fluorocarbon ferroelectrets with high piezoelectric coefficient. *Applied Physics A*. 2006; 84: 139-142. doi: 10.1007/s00339-006-3573-5.

131. Jung DH, Park IJ, Choi YK, Lee SB, Park HS, Rühe J. Perfluorinated polymer monolayers on porous silica for materials with super liquid repellent properties. *Langmuir*. 2002; 18(16): 6133-6139. doi: 10.1021/la025558u.

132. Li X, Cao Z, Liu F, Zhang Z, Dang H. A novel method of preparation of superhydrophobic nanosilica in aqueous solution. *Chemistry Letters*. 2006; 35(1): 94-95. doi: 10.1246/cl.2006.94.

133. Mahltig B, Böttcher H. Modified silica sol coatings for water-repellent textiles. *Journal of Sol-Gel Science and Technology*. 2003; 27(1): 43-52. doi: 10.1023/A:1022627926243.

134. Makita K, Akamatsu Y, Yamazaki S, Kai Y, Abe Y. Surface morphology of silica films derived by the sol-gel method and its application to a water repellent glass. *Journal of the Ceramic Society of Japan*. 1997; 105(1227): 1012-1017. doi: 10.2109/jcersj.105.1012.

135. Nakagawa T, Soga M. A new method for fabricating water repellent silica films having high heat-resistance using the sol-gel method. *Journal of Non-Crystalline Solids*. 1999; 260(3): 167-174. doi: 10.1016/S0022-3093(99)00594-3.

136. Rao AV, Kulkarni MM, Amalnerkar DP, Seth T. Superhydrophobic silica aerogels based on methyltrimethoxysilane precursor. *Journal of Non-Crystalline Solids*. 2003; 330(1-3): 187-195. doi: 10.1016/j.jnoncrysol.2003.08.048.

137. Rao AV, Pajonk GM, Bhagat SD, Barboux P. Comparative studies on the surface chemical modification of silica aerogels based on various organosilane compounds of the type R_nSiX_{4-n}. *Journal of Non-Crystalline Solids*. 2004; 350: 216-223. doi: 10.1016/j.jnoncrysol.2004.06.034.

138. Roig A, Molins E, Rodríguez E, Martínez S, Moreno-Mañas M, Vallribera A. Superhydrophobic silica aerogels by fluorination at the gel stage. *Chemical Communications*. 2004; 20: 2316-2317. doi: 10.1039/B407987F.

139. Shirtcliffe NJ, McHale G, Newton MI, Perry CC. Intrinsically superhydrophobic organosilica sol-gel foams. *Langmuir*. 2003; 19(14): 5626-5631. doi: 10.1021/la034204f.

140. Sosa S. Silica-based nanocomposite turns cotton into superhydrophobic fabric. *MRS Bulletin*. 2004; 29(12): 910-910. doi: 10.1557/mrs2004.253.

141. Ming W, Wu D, Van-Benthem RATM, De With G. Superhydrophobic films from raspberry-like particles. *Nano Letters*. 2005; 5(11): 2298-2301. doi: 10.1021/nl0517363.

142. Sun T, Wang G, Liu H, Feng L, Jiang L, Zhu D. Control over the wettability of an aligned carbon nanotube film. *Journal of the American Chemical Society*. 2003; 125(49): 14996-14997. doi: 10.1021/ja038026o.

143. Zhu L, Xiu Y, Xu J, Tamirisa PA, Hess DW, Wong CP. Superhydrophobicity on two-tier rough surfaces fabricated by controlled growth of aligned carbon nanotube arrays coated with fluorocarbon. *Langmuir*. 2005; 21(24): 11208-11212. doi: 10.1021/la051410+.

144. Erbil HY, Demirel AL, Avcı Y, Mert O. Transformation of a simple plastic into a superhydrophobic surface. *Science*. 2003; 299(5611): 1377-1380. doi: 10.1126/science.1078365.

145. Lu X, Zhang J, Zhang C, Han Y. Low-Density Polyethylene (LDPE) Surface with a Wettability Gradient by Tuning its Microstructures. *Macromolecular Rapid Communications*. 2005; 26(8): 637-642. doi: 10.1002/marc.200400626.

146. Wang DM, Lai JY. Recent advances in preparation and morphology control of polymeric membranes formed by nonsolvent induced phase separation. *Current Opinion in Chemical Engineering*. 2013; 2(2): 229-237. doi: 10.1016/j.coche.2013.04.003.

147. Xie Q, Xu J, Feng L, et al. Facile creation of a super-amphiphobic coating surface with bionic microstructure. *Advanced Materials*. 2004; 16(4): 302-305. doi: 10.1002/adma.200306281.

148. Mishra VK, Saini R, Kumar NA. review on applications of superhydrophobic coatings. *International Research Journal on Advanced Science Hub*. 2021; 3(3): 43-55. doi: 10.47392/irjash.2021.096.

149. Wang Y, Liu J, Li M, Wang Q, Chen Q. The icephobicity comparison of polysiloxane modified hydrophobic and superhydrophobic surfaces under condensing environments. *Applied Surface Science*. 2016; 385: 472-480. doi: 10.1016/j.apsusc.2016.05.117.

150. Subramanyam BS, Kondrashov V, Rühe J, Varanasi KK. Low ice adhesion on nano-textured superhydrophobic surfaces under supersaturated conditions. *ACS Applied Materials & Interfaces*. 2016; 8(20): 12583-12587. doi: 10.1021/acsami.6b01133.

151. Aparna A, Sethulekshmi AS, Saritha A, Joseph K. Recent advances in superhydrophobic epoxy based nanocomposite coatings and their applications. *Progress in Organic Coatings*. 2022; 166: 106819. doi: 10.1016/j.porgcoat.2022.106819.

152. Sutar RS, Gaikwad SS, Latthe SS, et al. nanocomposite coatings of hydrophobic silica NPs and poly (methyl methacrylate) with notable self-cleaning ability. In *Macromolecular Symposia*. 2020; Vol. 393, No. 1, p 2000116. doi: 10.1002/masy.202000116.

153. Ellis-Terrell C, Wei R, McKnight R, Huang X, Lin K. Thermal stability of superhydrophobic and oleophobic silica nanoparticle spray coating. *Materials Today Communications*. 2020; 25: 101370. doi: 10.1016/j.mtcomm.2020.101370.

154. Qian H, Zhu M, Song H, Wang H, Liu Z, Wang C. Anti-scaling of superhydrophobic poly (vinylidene fluoride) composite coating: tackling effect of carbon nanotubes. *Progress in Organic Coatings*. 2020; 142: 105566. doi: 10.1016/j.porgcoat.2020.105566.

155. Nguyen-Tri P, Tran HN, Plamondon CO, et al. Recent progress in the preparation, properties and applications of superhydrophobic nano-based coatings and surfaces: A review. *Progress in Organic Coatings*. 2019; 132: 235-256. doi: 10.1016/j.porgcoat.2019.03.042.

156. Selim MS, El-Safty SA, Abbas MA, Shenashen MA. Facile design of graphene oxide-ZnO nanorod-based ternary nanocomposite as a superhydrophobic and corrosion-barrier coating. *Colloids and Surfaces A: Physicochemical and Engineering Aspects*. 2021; 611: 125793. doi: 10.1016/j.colsurfa.2020.125793.

157. Selim MS, El-Safty SA, Fatthallah NA, Shenashen MA. Silicone/graphene oxide sheet-alumina nanorod ternary composite for superhydrophobic antifouling coating. *Progress in Organic Coatings*. 2018; 121: 160-172. doi: 10.1016/j.porgcoat.2018.04.021.

158. Donati M, Lam CWE, Milionis A, et al. Sprayable thin and robust carbon nanofiber composite coating for extreme jumping dropwise condensation performance. *Advanced Materials Interfaces*. 2021; 8(1): 2001176. doi: 10.1002/admi.202001176.

159. Ghashghaee M, Fallah M, Rabiee A. Superhydrophobic nanocomposite coatings of poly (methyl methacrylate) and stearic acid grafted CuO nanoparticles with photocatalytic activity. *Progress in Organic Coatings*. 2019; 136: 105270. doi: 10.1016/j.porgcoat.2019.105270.

160. Janowicz NJ, Li H, Heale FL, et al. Fluorine-free transparent superhydrophobic nanocomposite coatings from mesoporous silica. *Langmuir*. 2020; 36(45): 13426-13438. doi: 10.1021/acs.langmuir.0c01767.

161. Wang P, Yao T, Li Z, et al. A superhydrophobic/electrothermal synergistically anti-icing strategy based on graphene composite. *Composites Science and Technology*. 2020; 198: 108307. doi: 10.1016/j.compscitech.2020.108307.

162. Wang P, Wei W, Li Z, Duan W, Han H, Xie QA. superhydrophobic fluorinated PDMS composite as a wearable strain sensor with excellent mechanical robustness and liquid impalement resistance. *Journal of Materials Chemistry A*. 2020; 8(6): 3509-3516. doi: 10.1039/C9TA13281C.

163. Peng C, Chen Z, Tiwari MK. All-organic superhydrophobic coatings with mechanochemical robustness and liquid impalement resistance. *Nature Materials*. 2018; 17(4): 355-360. doi: 10.1038/s41563-018-0044-2.

164. Zhang X, Si Y, Mo J, Guo Z. Robust micro-nanoscale flowerlike ZnO/epoxy resin superhydrophobic coating with rapid healing ability. *Chemical Engineering Journal*. 2017; 313: 1152-1159. doi: 10.1016/j.cej.2016.11.014.

165. Zhao Z, Li X, Li W, et al. Progress in mechanism design of functional composites for anti-ice/deicing materials. *Surface Science and Technology*. 2024; 2(1): 2. doi: 10.1007/s44251-023-00033-2.

166. Wu Y, Dong L, Shu X, Yang Y, Feng P, Ran Q. Recent advancements in photothermal anti-icing/deicing materials. *Chemical Engineering Journal*. 2023; 469: 143924. doi: org/10.1016/j.cej.2023.143924.

167. Liu Z, Hu J, Jiang G. Superhydrophobic and photothermal deicing composite coating with self-healing and anti-corrosion for anti-icing applications. *Surface and Coatings Technology*. 2022; 444: 128668. doi: 10.1016/j.surfcoat.2022.128668.

168. Lin Z, Ma C, Ma Z, Gao L, Chen W, Chen G. Laser etching ultra-black coating with novel anti-icing performance. *Chemical Engineering Journal*. 2023; 466: 143067. doi: 10.1016/j.cej.2023.143067.

169. Yu B, Sun Z, Liu Y, Wu Y, Zhou F. Photo-thermal superhydrophobic sponge for highly efficient anti-icing and de-icing. *Langmuir*. 2023; 39(4): 1686-1693. doi: 10.1021/acs.langmuir.2c03384.

170. Lee SH, Kim J, Seong M, et al. Magneto-responsive photothermal composite cilia for active anti-icing and de-icing. *Composites Science and Technology*. 2022; 217: 109086. doi: 10.1016/j.compscitech.2021.109086.

171. Liu Y, Guo R, Liu J, Zhang Q. Robust PFMA/CNTs composite PDMS superhydrophobic film via SI-CuCRP method for efficient anti-icing. *Colloids and Surfaces A: Physicochemical and Engineering Aspects*. 2023; 660: 130913. doi: 10.1016/j.colsurfa.2022.130913.

172. Deng L, Wang Z, Niu Y, Luo F, Chen Q. CNTs-induced superhydrophobic and photothermal coating with long-term durability and self-replenishing property for anti-icing/de-icing. *Composites Science and Technology*. 2024; 245: 110347. doi: 10.1016/j.compscitech.2023.110347.

173. Liu X, Liu H, Li Y, Teng F, Liang C. Superhydrophobic surface of hybrid nanocomposites made of TiO_2 and multi-walled carbon nanotubes: Photothermal ice removal performance and wear resistance. *Applied Surface Science*. 2023; 640: 158318. doi: 10.1016/j.apsusc.2023.158318.

174. Huang J, Li D, Peng Z, Zhang B, Yao Y, Chen S. High-efficient anti-icing/deicing method based on graphene foams. *ACS Applied Materials & Interfaces*. 2023; 15(36): 43026-43037. doi: 10.1021/acsami.3c09360.

175. Chen J, Chen X, Hao Z, et al. Robust and superhydrophobic polydimethylsiloxane/ni@ $ti_3c_2t_x$ nanocomposite coatings with assembled eyelash-like microstructure array: a new approach for effective passive anti-icing and active photothermal deicing. *ACS Applied Materials & Interfaces*. 2024; 16(20): 26713–26732. doi: 10.1021/acsami.4c01561.

176. Cong Q, Qin X, Chen T, Jin J, Liu C, Wang M. Research progress of superhydrophobic materials in the field of anti-/de-icing and their preparation: a review. *Materials*. 2023; 16(14): 5151. doi: org/10.3390/ma16145151.